STUDY ON THE THERMODYNAMICS AND KINETICS OF THE STRIPPING OF PALLADIUM FROM A TYPICAL PALLADIUM ORGANIC

A thesis submitted to the faculty of
ENGINEERING AND THE BUILT ENVIRONMENT
of the
UNIVERSITY OF CAPE TOWN
in Fulfilment of the Requirements of the Degree of
MASTER OF SCIENCE IN ENGINEERING

By
Johannes Hendrik Wilhelmus Machiel Brits
B.Eng. (Chemical Engineering) University of Pretoria

Mineral Processing Research Unit
University of Cape Town
Rondebosch 7700
South Africa
March 2005

Abstract

The aim of this thesis was to investigate the thermodynamics and the kinetics of the stripping of palladium from a typical palladium organic. The thesis firstly characterizes the thermodynamic effects of temperature and strip acid normality on the stripping of palladium and secondly investigates the kinetics of the palladium stripping reaction by exploring the effect of impeller speed and type on the overall volumetric mass transfer coefficient, which was the major focus of this thesis.

The test work for this thesis was performed at the Anglo American Research Laboratories (ARC) in Johannesburg, South Africa. The test work was performed using a 1/5 scale pilot plant mixer-settler that was designed and built according to the Anglo Platinum Precious Metals Refiners' (PMR) palladium stripping mixer-settler design drawings. All tests were performed using filtered aqueous feed from the PMR, but the palladium organic was prepared from its constituents to prevent degradation products or organic contamination that may be prevalent in the PMR solvent extraction circuits from influencing the test work results.

Fifteen experiments were performed to characterize the palladium stripping reaction in terms of operating temperature and strip acid normality. Another six experiments were performed to generate an equilibrium isotherm under the optimum conditions for the hydrodynamic characterization experiments.

In addition to the palladium stripping characterization experiments, hydrodynamic characterization experiments were done at various settings of impeller speed using a 4-bladed radial disc impeller and a Rushton turbine. The data from these experiments was used to evaluate hydrodynamics such as power input and power intensity, mixing and organic-aqueous dispersion.

Palladium stripping rate was found to increase with temperature and strip acid normality. The stripping rate also increases with an increase in impeller speed and power intensity as is commonly found in solvent extraction literature. Experiments performed with a Rushton turbine, at equivalent power intensities (lower RPM) to that of a 4-bladed radial disc impeller, resulted in a 20% decrease in mixer vessel volume due to excessive air entrainment because of vortexing. The overall volumetric mass transfer coefficient was found to increase with an increase in impeller speed until excessive air entrainment causes the volumetric mass transfer coefficient to decrease.

The thesis concludes that the stripping of palladium is mass transfer limited over the entire range of power intensities investigated. Therefore stripping kinetics can be improved by increasing impeller speeds of industrial mixer-settler applications.

Acknowledgements

I would like to express my sincere thanks to my supervisor, Dr Dave Deglon, for his invaluable advice and guidance in this study.

The help of the following people is also gratefully acknowledged:

My co-supervisor, Professor Peter Gaylard, for his encouragement and enthusiasm.

The staff at Anglo Platinum for their financial assistance and assistance with the pilot plant design, manufacturing and trials; in particular Harald Muller, Deborah Craig, Karen Viljoen, Malcolm Arendse, Dr. Victor Mtotywa, Dr. Stephen Woollam and Richard Grant.

Peter Charlesworth and the management of the Anglo Platinum Precious Metals Refiners for their assistance and support of this study towards a Masters degree of Science in Engineering.

My wife, Kim, for her eternal patience and encouragement during the past two years and my newborn son, Alex, for waiting patiently for my return to home over weekends.

But most of all to the Lord Almighty for granting me this opportunity and wisdom to succeed.

TABLE OF CONTENTS

List of Figures

List of Tables

Nomenclature

δ	Effective thickness of stagnant-film layer
ε	Specific power input
$(\varepsilon_T)_{max}$	Maximum local energy dissipation rate
$(\varepsilon_T)_{imp}$	Impeller local energy dissipation rate
ϕ_{aq}	Aqueous volume fraction
ϕ_{org}	Organic volume fraction
μ_{aq}	Aqueous viscosity
μ_{org}	Organic viscosity
μ_M	Mean viscosity
ρ_{aq}	Aqueous phase density
ρ_{org}	Organic phase density
ρ_M	Mean density
τ	Residence time
τ_c	Average circulation time (time for the volume of the tank to be circulated by the impeller)
a	Liquid-liquid interfacial area per liquid volume
A	Interfacial area
B	Number of blades on the impeller
C	Impeller height above the bottom of the tank
$C_{b,o}$	Bulk organic phase concentration
$C_{b,a}$	Bulk aqueous phase concentration
$C_{s,o}$	Organic concentration at the interface
$C_{s,a}$	Aqueous concentration at the interface
ΔC	Concentration difference between bulk solution and interface
D	Impeller diameter
D_c	Distribution coefficient
D_L	Liquid phase diffusion coefficient
e	Power intensity
e_{imp}	Impeller power intensity
e_{gas}	Gas power intensity
g	Gravitational forces
H	Liquid depth
j	Flux across an interface

J	Baffle width
k_L	Mass transfer coefficient
K_La	Overall volumetric mass transfer coefficient
k_a	Aqueous phase mass transfer coefficient
k_o	Organic phase mass transfer coefficient
K_c	Settling rate coefficient
K_{eq}	Equilibrium constant
L	Length of impeller blade
N	Impeller rotational speed
N_P	Power number
N_{Fr}	Froude number
N_{Re}	Impeller Reynolds number
N_q	Flow number
N_h	Head number
P	Impeller power consumption
Q_{aq}	Aqueous flow rate
Q_{org}	Organic flow rate
Q	Total flow rate (Organic and aqueous)
R_a	Reaction rate
R	Number of baffles
s	Fractional surface renewal rate
S	Pitch of the impeller
S_{area}	Settler area
t	contact time
T	Tank diameter
u'	Fluctuating velocity
U_{tip}	Impeller tip speed
V	Mixer vessel volume
V_{eff}	Effective volume for mass transfer
V_{aq}	Aqueous volume in mixer
V_{imp}	Impeller swept volume
W	Width of impeller blade

Abbreviations

PGM	Platinum group metals
RPM	Revolutions per minute
RTD	Residence time distribution
UCT	University of Cape Town
PMR	Anglo Platinum Precious Metals Refiners
TBP	Tributyl-Phosphate

1 Literature Review

This chapter presents a review and critique of the literature pertaining to the topics dealt with in this thesis. The chapter firstly presents a brief overview of the process of solvent extraction; the stripping of palladium from palladium loaded organic and then discusses mixer-settlers. An overview of mass transfer in liquid-liquid dispersions is given where after the chapter concludes with a review of dimensional analyses and hydrodynamic effects in mixer-settlers after which the scope and objectives of the thesis are presented.

1.1 Solvent Extraction

1.1.1 Overview of Solvent Extraction

Solvent extraction (SX) or liquid-liquid extraction involves the extraction of a constituent from an aqueous phase into an organic phase, and usually the subsequent stripping of this component back into a different aqueous phase in a purified and concentrated form (Fox, 1994). This unit process is used to either remove an impurity from a process stream or to remove the valuable component from the stream for further purification, leaving the impurities in the original aqueous phase. Scrubbing and stripping sections may be added to the circuit to enhance the performance of the unit process. Scrubbing stages removes the majority of co-extracted constituents and also buffers the extraction stages from the stripping stages by removing any entrained impurities and aqueous phase from the organic phase. Wash / reconditioning stages after the stripping section are usually installed to remove any acid from the organic phase and to recondition the organic before recycling it to the front end of the SX circuit.

1.1.2 Solvent Extraction in the PGM Industry

Solvent extraction is a technique that uses the phenomenon of distribution between two liquid phases to separate the components of a solution. Fifty years ago, solvent extraction was employed mainly as an analytical tool to separate elements with closely related chemical properties. The discovery and isolation of the lanthanide and actinide elements provided further momentum for the development of SX technology (Nash, 1993). SX technology was pioneered during the Second World War (Manhattan Project) for the recovery of uranium from primary ores and this led to the recovery of uranium and plutonium from spent reactor fuel (Sole, 1999; Cole, 1994). Since then

developments have taken place in a broad field of applications, from analytical chemistry to large scale industrial processes such as the pharmaceutical and base metal industries. Although one of the earliest examples of counter-current SX was the extraction of acetic acid over 100 years ago, the use of SX has only advanced significantly over the past 50 years (Cole, 1994).

Today, SX is widely employed in a variety of industries for both upgrading and the purification of a suite of elements and chemicals. These include large copper plants treating up to 120 000 m^3 of solution per day (Kennedy, 1999) and precious metals SX refining processes treating only a few liters per hour (Mooiman, 1993).

Until fairly recently, the refining of precious metals relied heavily on the classical methods of precipitation and selective dissolution, which are extremely tedious and inefficient (Cole, 1994). These inefficiencies are mainly due to the substantial number of recycles required as well as the large number of solid-liquid separations and the associated residence times and pipeline of the circuits. High refining costs are inherent to these conventional processes (Edwards, 1975). However, in the past two decades, there have been significant advances in the processing of these elements and solvent extraction is now widely used as the primary separation technique (Sole, 1999). Details of most of these commercial processes remain closely guarded secrets of the industry, but some outlines of the processes have been published (Flett, 1982). These include the organic extractants used for palladium (Sole, 1999):

- Dioctylsulphide – Inco Precious Metals Refinery (Rimmer, 1989; Barnes, 1982)
- Di-n-hexylsulphide – Lonrho's Western Platinum Refinery (postulated) (Harris, 1993; Renner, 1985)
- β-hydroxyoxime – Anglo Platinum and Johnson Matthey (UK) (Mooiman, 1993)

Another extractant that can be used is:

- Dialkylsulphoxides (Preston and du Preez, 2002)

Solvent extraction processes can be classified mainly in three categories (Mooiman, 1993):

- Solvating extractants (long chain alcohols, ethers and TBP)
- Anion-exchange extractants (long-chain alkylamines), and
- Coordination extractants (oximes and dialkylsulphides)

1.1.2.1 Stripping / Reverse Extraction using Oximes

Oximes are well established extractants for palladium and their use has been extensively studied and patented (Reavill and Charlesworth, 1980; Cleare *et al*, 1979; Shanton and Grant, 1982). The oximes, which are selective for Pd, are those of the α-hydroxyoxime, the hydroxyphenyl oxime and the alkoxyphenyl oxime type. Another reagent, 8-Hydroxyquinoline, has also been studied extensively. These are similar and in some cases the same oximes that are used commercially for copper solvent extraction. The general chemical structures that will extract palladium are shown in Figure 1.1 below.

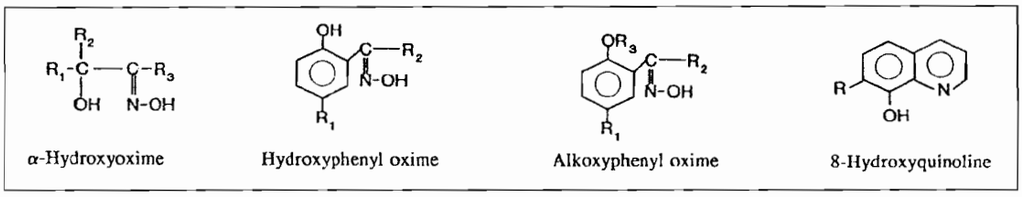

Figure 1-1 Chemical structures of oxime reagents (Mooiman, 1993).

The oximes, except for the latter, have a high selectivity for Pd and function like the dialkyl sulphides by a ligand substitution mechanism. The extraction kinetics, particularly for the hydroxyphenyl and alkoxyphenyl oximes are slow. The addition of amines may accelerate the extraction reaction and stripping can be done with high acid concentrations (Reavill and Charlesworth, 1980).

Flett *et al* (1983) tabled the structures and properties of various chelating extractants such as P5100 and LIX 65N as well as oxime derivatives such as Kelex 100 in their discussion on commercial solvent systems for inorganic processes.

The reaction for the extraction of Pd from the aqueous HCl solution onto the oxime organic can be simplified as follows (Grant *et al*, 1998):

$$[PdCl_4]^{2-} + 2RH \leftrightarrow [PdR_2] + 4Cl^- + 2H^+ \qquad (1.1)$$

where RH represents the protonated oxime

$$K_{eq} = \frac{[[PdR_2]]\,[Cl^-]^4[H^+]^2}{[[PdCl_4]^{2-}]\,[RH]^2} \tag{1.2}$$

based on activities

$$D_c = \frac{[[PdR_2]]}{[[PdCl_4]^{2-}]} \tag{1.3}$$

and by rearranging Equation 1.2

$$D_c = \frac{[[PdR_2]]}{[[PdCl_4]^{2-}]} = K_{eq}\frac{[RH]^2}{[Cl^-]^4[H^+]^2} \tag{1.4}$$

Factors that influence the stripping reaction (thermodynamics) are therefore:

- $[PdCl_4]^{2-}$ concentration
- oxime concentration
- Cl^- concentration
- H^+ concentration
- temperature

Renner (1985) highlighted that the rate of reaction is a function of the following parameters:

- Mixing parameters
- $[PdCl_4]^{2-}$ concentration
- oxime concentration
- Cl^- concentration
- H^+ concentration
- temperature

1.1.2.1.1 Extraction Efficiency

In the case of acid chelating extractants, the change in the acidity of the aqueous solution is responsible for the extraction or stripping of the metal ion. Increasing the pH of the solution thus increases the extraction and decreasing the pH promotes stripping or back extraction. Changing the

pH of the system allows for the distribution of the metal between the organic phase and the aqueous phase to be adjusted.

For this type of system where the extraction of a metal ion is pH dependent, a set of pH versus extraction / stripping curves can be generated for the various elements present in the organic. These curves allow the determination of an optimum operating pH and the selectivity characteristics of the solvent system. The curves are generated by contacting known quantities of the solvent and feed solution and adjusting the pH of the system to certain values. The organic and aqueous can then be sampled and analyzed after reaching equilibrium. A mass balance over the system can be performed and the pH versus extraction curves generated.

Repeating the above experiment at a different temperature will allow the effect of temperature on the system to be examined (Nagel, 1999). Temperature can have a considerable effect on the extraction and stripping properties of a solvent extraction system with respect to equilibrium, kinetics and metal separations. This is especially the case if high metal loadings are obtained in the solvent (Ritcey and Ashbrook, 1979b).

1.1.2.1.2 Equilibrium Isotherms

Before the stripping isotherms can be constructed, the organic needs to be loaded to a predetermined concentration of the metal ion. A stripping isotherm is generated by contacting organic and strip acid together at different O:A ratios at the optimal operating pH and temperature required (Bridges and Rosenbaum, 1962; Nagel, 1999). The pH of each contact must be adjusted to the desired pH and maintained there until the system reaches equilibrium. Samples of both phases are then analyzed and stripping equilibrium isotherms constructed. A McCabe-Thiele construction can then be plotted on the isotherm to determine the number of stripping stages required at a specific O:A ratio.

1.1.2.1.3 Stripping Kinetics

Knowledge about the reaction kinetics of a solvent extraction system is important to ensure adequate reaction time and for the design of the mixers required for full scale operation. The sizing of the mixing vessel is directly influenced by the reaction kinetics of the solvent extraction system. The faster the kinetics, the smaller the mixer vessel has to be for a set organic and strip feed rate. There are numerous methods available for the determination of the reaction kinetics of a system:

- One method involves the mixing of the two phases together at the chosen temperature and pH. Samples from the mixer vessel are drawn at regular intervals, phase separated and analyzed.
- An alternative method is to contact different batches of the two phases for a variety of time intervals.
- Another method is to mix the two phases in a small-scale mixer-settler. By varying the flow rates of the two phases, the residence time in the mixer vessel can be varied. The phases exiting the mixer vessel can then be sampled from the settler, analyzed and the extraction achieved plotted as a function of the contact time in the mixer vessel (Nagel, 1999). This method also enables one to analyze settler phase disengagement and entrainment within the same experiment.

In heterogeneous systems such as we have in solvent extraction, the rate of extraction of a metal will depend largely on the surface area of the dispersed phase. One should note that in a contactor one phase will be dispersed (dispersed phase) in the other (continuous phase) and this depends largely on the conditions initially present at the start of agitation of the phases. The surface area of the dispersed phase will depend on the amount of agitation: that is the energy input into the system. However, it should not be thought that the greater the agitation, the greater the rate of metal extraction. Too much energy input can result in the formation of stable or semi-stable emulsions. Furthermore, decreasing the droplet size of the dispersed phase can result in the making of droplets resembling rigid droplets. In this condition there is no internal movement within the droplets, no new surfaces are produced and the extractant within the droplet cannot get to the surface to react with metal ions. Consequently the reaction rate is slow (Ritcey and Ashbrook, 1979a).

1.1.2.1.4 Chemical Rate Limiting vs. Mass Transfer Rate Limiting

As with all processes, the slowest step is rate limiting, that is, it controls the overall rate of the reaction. Generally, metal extraction is governed by mass transfer and diffusion rates which for reactions involving chelates can vary over a considerable range (Ritcey and Ashbrook, 1979a). This means that increased mixing intensity could increase the reaction rate, but up to a point where the chemical reaction may become rate limiting.

From the previous sections it is clear that the extraction of palladium is done via coordination / chelation chemistry by the refineries highlighted in Section 1.1.2 and therefore warrants an overview of the sub processes applicable to such circuits.

1.1.3 Sub Processes of Solvent Extraction

Solvent extraction as a unit operation consists of at least two sub processes, which include extraction and stripping. The circuit may however have more sub processes depending on the nature of the extractability of the impurities or constituents and the nature of the organic used to do the separation. An additional scrub section may be incorporated in the overall layout to scavenge co-extracted constituents from the organic back into the scrub aqueous and prevent them from entering the stripping section. A wash or regeneration circuit could also be added to wash the organic in order to remove any entrained acid or constituents, which could result in organic degradation. The regeneration circuit may also be necessary to regenerate the organic before recycling back to the extraction stage. In general, SX circuits are operated in a counter-current manner with the aqueous and organic streams flowing in opposite directions to maximize the extraction and (or) stripping efficiencies. The following schematic shows the layout and process stream flows of a generalized solvent extraction plant.

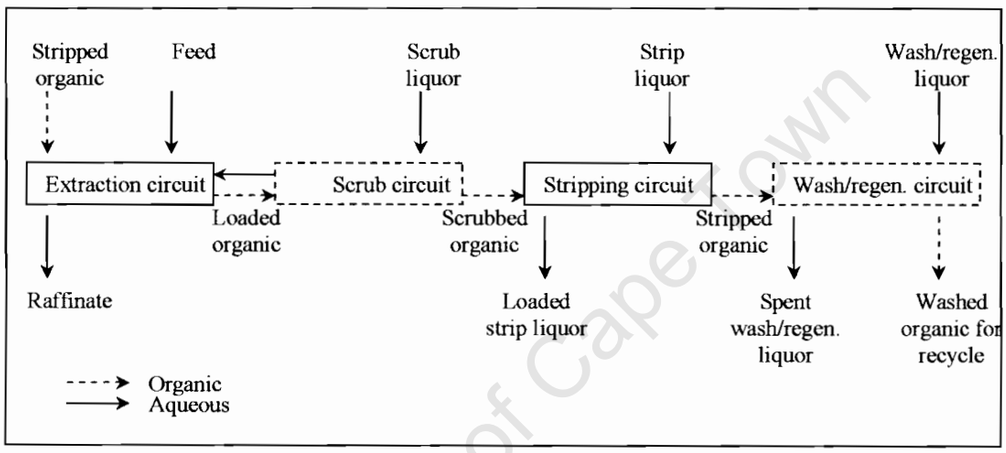

Figure 1-2 Generalized solvent-extraction circuit (Sole, 1999).

1.1.3.1 Extraction

The objective of the extraction circuit is to selectively load a chemical species (valuable element or impurity) without co-extracting appreciable amounts of unwanted species. This requires that an appropriate organic is chosen that is selective towards the species that needs to be extracted. This also necessitates that the feed preparation is done correctly to ensure that the elements are in the correct chemical form (species). Pre conditioned feed (correct redox potential, acid strength and metal concentrations) is contacted with stripped organic and the required species loaded onto the organic. The "barren" aqueous stream, depleted of the metal being loaded onto the organic, then

leaves the extraction circuit as raffinate. The loaded organic is then forwarded to the scrubbing section.

1.1.3.2 Scrubbing

The loaded organic from the extraction circuit is counter currently contacted with scrub solution to scrub any weakly co-extracted species from the organic into the aqueous. This section also removes any entrained aqueous from the extraction section and acts as a buffer between the extraction and stripping circuits to minimize the deportment of impurities to the strip aqueous stream. The scrubbed organic then flows to the stripping section.

1.1.3.3 Stripping

The loaded organic from the extraction circuit (via scrub circuit) is counter currently contacted with strip solution to strip the valuable species from the organic. Invariably loaded species that were not scrubbed from the organic during the scrub stages might also be stripped from the organic during the strip stages. The co-stripped impurities need to be removed from the loaded strip liquor by further treatment. The stripped organic then flows to the wash section for further treatment.

1.1.3.4 Washing

The stripped organic, containing very low concentrations of the valuable metal, is then treated in the wash section. The stripped organic is counter currently contacted with water or wash solution for two reasons. The first is to remove any entrained aqueous from the organic in order to prevent strong acid from entering the extraction circuit due to the recycling of the organic from the strip circuit back to the extraction circuit. The second reason for washing the organic is that the organic is susceptible to degradation when in contact with strong acid for extended periods of time and therefore needs to be washed to remove any entrained hydrochloric acid. The washed organic is then recycled back to the extraction stages.

1.1.4 Overview of Solvent Extraction Equipment

The most commonly used solvent extraction contactors in the metallurgical industry are box-type mixer-settlers. These are relatively inexpensive devices and are simple to operate. Other contactors include pulsed columns, mechanically agitated columns and centrifugal contactors. To ensure that good mass transfer of the extracted or stripped species occurs across the organic-aqueous interface,

it is necessary to provide adequate contact between the two phases. It is therefore necessary to be familiar with the chemical and physical properties of the extraction system, in order to be able to specify which contactor may be appropriate. Fox (1994) and Mooiman (1993) highlighted some factors, which influence the choice of contactor type. These are:

- number of stages required for each section
- volumetric throughput
- kinetics of extraction / stripping (residence times required)
- relative phase ratio
- the need for pH control
- corrosivity of the aqueous phase
- available space
- value of the product contained in the solution inventory
- stage efficiency requirements
- phase dispersion and disengagement rate.

The choice of contactor type would also have to take the following into account:

- capacity to handle crud
- capacity to handle solids
- ease of operability and adaptability to process changes such as concentrations and flow rates

Each contactor type will be briefly discussed in the next section.

1.1.4.1 Mixer-settlers

Mixer-settlers are usually operated in a counter-current configuration, but are sometimes run in a co-current configuration particularly with extraction systems with slow kinetics. The contact between the organic and aqueous phases is discontinuous and takes place in discrete steps. Separation of the phases takes place between each of the steps (contacts) and each contact and separation is called a stage (Sole, 1999).

The aqueous and organic phases are drawn into the mixing vessel from the adjacent units by a pumping impeller. In the mixing vessel, the two phases are mixed for sufficient time to allow mass transfer to take place. The use of a pumping impeller obviates the need for separate pumps for interstage solution transfer. The mixed phase then overflows into the settling vessel, where the two phases disengage under the influence of gravity. The organic phase overflows the top weir, while

the aqueous phase is removed via a barometric leg. The adjustable barometric leg allows the height of the interface in the settler to be varied (Fox, 1994).

Mixer-settlers are usually preferred for systems in which there is poor phase disengagement and a considerable settling area is required. Stage efficiencies in this configuration are high. Interstage pH control, if necessary, in mixer-settlers is easier than in columns. Solvent extraction equipment vendors such as Krebs, Davy International and Outokumpu have developed several variations on this basic design. The trend is to use multiple mixers with two or more mixing vessels, which gives improved mass transfer per stage without over mixing since over mixing causes excessive organic entrainment (Sole, 1999). A typical box type mixer-settler is illustrated in Figure 1.3.

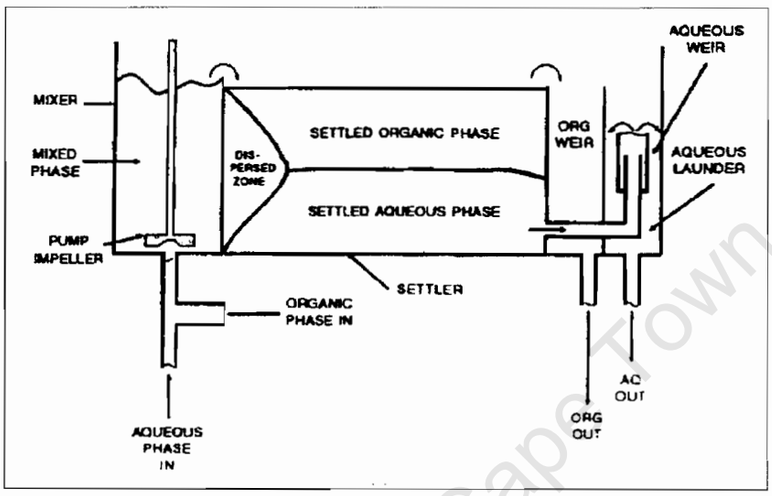

Figure 1-3 Conventional mixer-settler unit (Fox, 1994).

1.1.4.2 Column Contactors

Unlike mixer-settlers, column contactors allow the contact of the two phases to be continuous over the all the stages. There are four main types of columns:

- reciprocating-plate columns
- pulsed columns
- packed columns
- agitated columns

The reciprocating columns consist of a stack of perforated plates and baffles, supported by a central reciprocating shaft, which is driven by an external mechanism above the column. The power input into the system can be varied by varying the amplitude and reciprocating speed of the reciprocating shaft. For these types of contactors, the light phase is introduced at the bottom of the column and the heavy phase at the top. Columns are usually operated with the organic as the dispersed phase to reduce organic inventory and also for safety reasons.

Pulsed columns operate in exactly the same way as the reciprocating columns except for the agitation, which is provided by the reciprocating pulsation action of the solutions rather than the movement of column internals. A pulsed configuration designed by Bateman is illustrated in Figure 1.4.

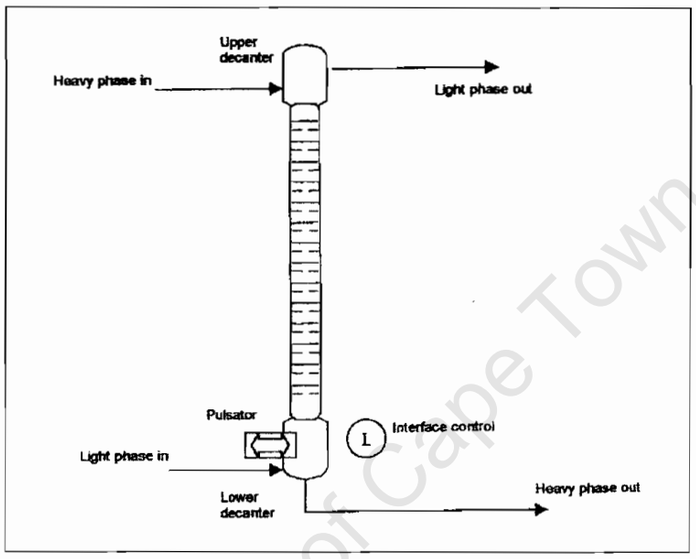

Figure 1-4 Bateman pulsed column (Fox, 1994).

In packed columns there is no external mechanism to agitate the phases and mass transfer results from the turbulence created by the hydrophilic or hydrophobic packing.

Stirred columns on the other hand make use of a central shaft with rotors to agitate the two phases between the perforated plates. A typical stirred column is illustrated in Figure 1.5.

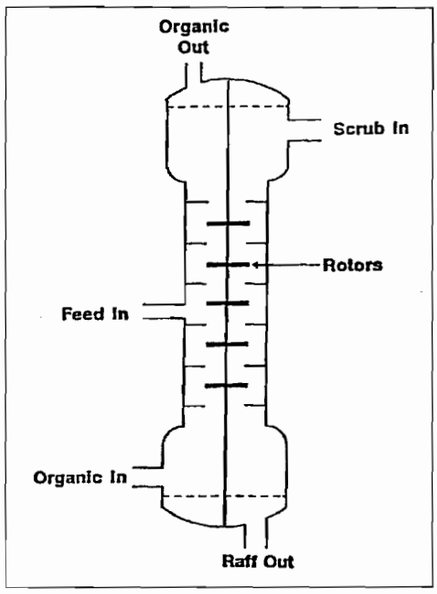

Figure 1-5 Typical stirred column (Grant *et al*, 1998).

Columns are very useful for processing low flow rates and for systems in which there is a tendency for emulsification. A large number of stages can be provided in a single column and columns take up very little floor space, but needs considerable headroom. Another advantage of columns is that the extraction and stripping processes occur in a closed system. This is especially valuable for toxic processes and processes requiring an inert atmosphere due to the possibility of fire (Sole, 1999).

1.1.4.3 Centrifugal Contactors

Centrifugal contactors usually involve the combination of a high-speed impeller and centrifugal separator in a single unit. Several different designs are available from manufacturers such as Robatel and Alva-Laval. The main advantages of these units are their fast kinetics and very low solution hold-up. This has distinct advantages for systems in which low organic inventories are required. They are not appropriate for systems in which long residence times are required or for low flow rates (Mooiman, 1993). A Robatel centrifugal contactor is illustrated in Figure 1.6.

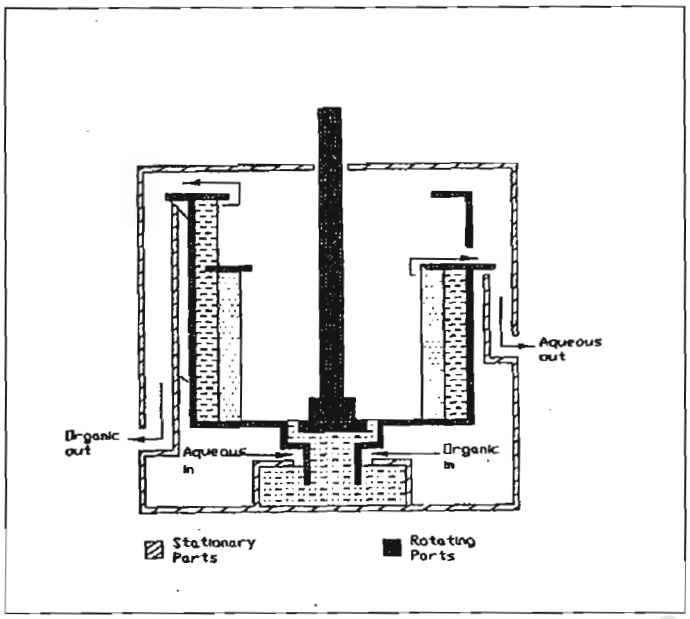

Figure 1-6 Robatel centrifugal contactor (Mooiman, 1993).

1.2 Mixer-settlers

As indicated earlier, mixer-settlers are currently by far the most common type of solvent extraction equipment. The major mixer-settler manufacturers have all made modifications to the conventional mixer-settler design to improve mixing and settling, but these mixer-settlers still have the same basic features and fulfil the same basic function. Mixer-settlers are used not only in very large copper extraction plants, but also in relatively small precious metals SX plants such as the Anglo Platinum Precious Metals Refiners plant in Rustenburg, South Africa. Because of their common use in solvent extraction plants and because this thesis is based on work performed using a mixer-settler, mixer-settlers will be discussed in greater depth in this section. A basic overview of mixer-settlers will be given and differences between the most common mixer-settler types will be highlighted.

1.2.1 Types of Mixer-settlers

Solvent extraction (SX) has been used to extract metals for a long time. In the late 1960's, the popular and accepted Holmes & Narver pump mixer design was introduced to recover copper. With time, four other solvent extraction designs surfaced: Davy, Bateman, Outokumpu, and Krebs. The former all have the same mixer-settler concept: one impeller in the first chamber or tank creates the flow and initial dispersion, other impellers maintain the dispersion long enough for the

mass transfer to take place, and a settling zone separates the aqueous from the organic phases. This is illustrated in Figure 1.7. Krebs has reversed the order with mixing first and pumping second (Post, 2003).

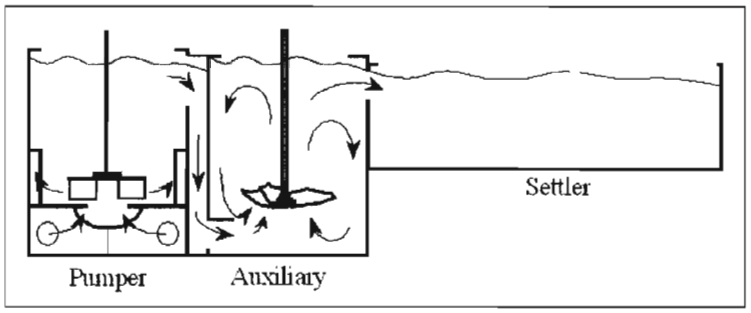

Figure 1-7 A mixer-settler overflow schematic showing the pumper and auxiliary mixing stages, followed by a settler of a conventional SX-circuit (Post, 2003).

Another design is the dual impeller pumper, which has a pumper and a mixer impeller on the same shaft in one mixer vessel (Post, 2003) as illustrated in Figure 1.8.

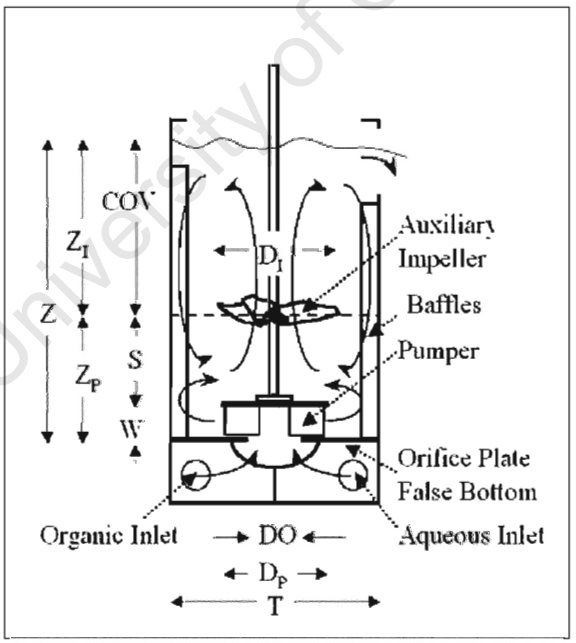

Figure 1-8 Schematic of a dual impeller pump stage (Post, 2003).

The optimal design has now migrated away from square boxes to cylindrical tanks, which are now used in all designs.

1.2.2 Mixer-settler Design Variations

Although most of the mixer-settlers discussed in the previous section are similar in general layout, each has its own characteristic variation from the conventional mixer-settler design. A few of the most obvious differences are stated for the mixer-settlers previously mentioned. These include:

- Open conventional systems will entrain air from the surface. Outokumpu recognizes this problem and installs surface covers to eliminate the air induction.
- The auxiliary stage must be designed to maintain the initial dispersion at a minimum of extra shear. Good mixing is important with high flow, to minimize short-circuiting and maximize contact time of the two phases. If the mixing isn't designed right, phase separation can already occur here and cause increased head requirements on the pumper, which will restrict the flow. Lightnin uses up-pumping axial hydrofoils for this purpose, while Outokumpu uses the Spirok and Krebs uses a pitched bladed turbine. These impellers are shown in Figure 1.9.

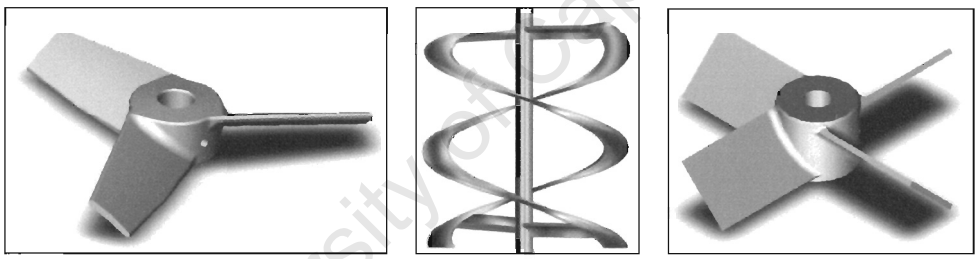

Figure 1-9 Schematic of an axial hydrofoil, dual spiral impeller (similar to Spirok) and pitched blade turbine (Post, 2003; Cole, 1994).

1.2.3 Sub Processes in Mixer-settlers

To be able to operate and design a solvent extraction mixer-settler plant it is essential to have knowledge of some of the sub processes, which take place inside the mixer vessel as well as the subsequent settler. The following section provides a brief overview of the important sub processes of hydrodynamics, liquid-liquid dispersion as well as phase separation. These sub processes are explored in more detail in Section 1.5, which focuses on the effects of the key "hydrodynamic" variables such as impeller speed and type on these sub processes.

1.2.3.1 Hydrodynamics

Hydrodynamics refers to the flow of fluid in a mixer vessel and settler and is largely driven by the action of the impeller. Many types of impellers are used to produce shear and mixing in the mixing vessel of a mixer-settler. Most mixing is done by means of a rotary impeller and therefore three velocities exist within the liquids being mixed. These velocities are classified as radial (outward from the axis of rotation), longitudinal or axial (along the direction of the rotor shaft) and tangential. For successful mixing, both the radial and longitudinal velocities need to be optimized by the use of baffles or by the positioning or orientation of the impeller.

To produce mixing, it is required to supply energy to the fluid by means of the rotation of an impeller. The rate at which the energy is supplied, not only depends on the type of agitator used and the speed at which it rotates, but also the physical properties of the fluid, shape of the vessel and baffles. To characterize the behaviour of any impeller, it is therefore necessary to take into consideration the complete environment in which it operates.

The function of a rotating impeller is to produce movement of the fluid and eddy currents are produced as a result of this action. The established flow patterns influence key hydrodynamic parameters such as the organic-aqueous dispersion and the residence time distribution. The flow pattern created in mixers is governed by vessel characteristics, such as size, shape and baffles, and impeller properties such as shape, diameter, rotational speed, position off bottom, and liquid depth. Knowledge of the hydrodynamic aspects of a mixer's operation enables the designer to appreciate the various influences of the key variables mentioned above when not only designing a mixer-settler, but also when scaling up from a pilot plant operation.

In most mixer-settler applications very high impeller Reynolds numbers are obtained, indicating a fully turbulent flow regime. Turbulence in mixing vessels is normally treated at a "bulk level", through parameters such as the Reynolds number, impeller tip speed and power input. Turbulent conditions (and therefore improved mixing) occur at high Reynolds number values, and this is largely brought about by increases in the impeller speed.

The impeller creates a dispersion of the organic and aqueous phases. The appropriate power level and impeller type create the proper head, flow, droplet dispersion and phase stability. If too little power is applied, phase disengagement takes place, greatly reducing the interfacial area available for mass transfer. If too much power is applied, surface splashing and air entrainment occur, contributing to crud formation (Yantz, 2000).

1.2.3.2 Organic - Aqueous Dispersion

Dispersion in a mixer vessel refers to the ability of a mixer vessel to create an organic-aqueous dispersion that is conducive to mass transfer of valuable species between the two phases. In order for mass transfer to take place between the two phases, a large surface area needs to be created. Without this large surface area, the overall process would become mass transfer rate limiting. As the two phases enters the mixing vessel and accumulates in the low-pressure regions behind the rotating impeller blades, droplets are sheared off by the action of the impeller. It is this shearing action that is responsible for the creation of very small organic in aqueous droplets or aqueous in organic droplets depending on which phase is the continuous phase. Further droplet breakage occurs in the turbulent conditions in the impeller zone and droplets are dispersed into the mixing vessel by the bulk fluid flow caused by the pumping action of the impeller. In the bulk region of the vessel droplets may collide and coalesce, recirculate back to the impeller region, descend under gravity or rise to the top due to density differences.

The organic-aqueous dispersion is the single most crucial parameter within a mixer-settler since it has the most profound influence on not only the distribution of the desired species between the organic and aqueous phases, but also the physical characteristics when it comes to the settler and the required phase disengagement therein. Without proper dispersion, inadequate contact between organic and aqueous phases results and therefore the efficiency of the solvent extraction process is dramatically reduced.

Impeller speed is of vital importance to organic-aqueous dispersion. When the mixed phase enters the impeller region, it is the action of the impeller that controls organic-aqueous dispersion and the consequent droplet size. Increasing the impeller speed leads to smaller droplets, which improves the rate of solvent extraction mass transfer. It is well known that the geometry and scale of the vessel and impeller, agitation rate as well as the physical properties of the mixed phases, determine the breakage and coalescence rates and resulting drop size distributions.

It is important to run the impeller at speeds above the lower critical speed to prevent phase disengagement to occur within the mixer vessel and therefore a change in phase hold-up ratio. This change in phase hold-up ratio may cause a continuous phase inversion.

In applications where dispersion is required, turbines are most often used followed by propellers and very rarely paddle type impellers (Sandler and Luckiewicz, 1987).

1.2.3.3 Phase Disengagement

The final process of solvent extraction within a mixer-settler is the separation of the two phases that were mixed in the mixer vessel. During this stage, the droplets created in the mixing vessel coalesce to form bigger drops and eventually separates into two phases. If the mixing by the impeller is too intense, very small droplets could be formed that could not coalesce fast enough under gravity in the residence time of the settler. In the extreme situation, a stable emulsion may even form, rendering the settler non operational and forcing the plant to shut down. There is therefore a fine balance between achieving a very good dispersion for maximum mass transfer and fast kinetics and creating a dispersion that is either very slow to settle or in the worst case a stable emulsion.

Nagel (1999) highlighted that a settler is normally chosen (based on industry standards) which generates a dispersion band depth of approximately 10-15% of the settler depth and that the corresponding settling rate coefficient is calculated according to Equation 1.5 in $m^3/(m^2.hr)$

$$K_c = (Q_{aq} + Q_{org}) \frac{60}{S_{area}} \tag{1.5}$$

Charlesworth (1981) highlighted that the thickness of the dispersion band depends on a number of factors including the mixing conditions, the composition of the phases and the flow rates.

Another issue related to dispersion is the concept of phase stability. Nienow (2004) indicated that two simple rules have been reported when it comes to phase stability:

- If either phase is < 30% v/v it will be dispersed
- If an agitator is started in a phase, it tends to be continuous.

What must be noted though is that although an agitator may be started in one phase (rule 2), after some time rule 1 may take over leading to inversions due to coalescence.

Reeve and Godfrey (2002) states that in mixer-settler applications a specific continuity is often preferred for reasons of lower entrainment in the coalesced phases leaving the settler. When the organic/aqueous flow ratio is high (80-90%) only organic continuous operation is possible. Conversely, at low flow ratios (20-40 %) only aqueous continuous operation can be achieved. At intermediate ratios either continuity can be achieved. A decrease in rotational speed reduces the stability of organic continuous dispersions.

Hydrodynamics, dispersion and coalescence are strongly influenced by the two key hydrodynamic variables of impeller speed and type. These two variables have an enormous effect on each of the sub processes occurring in a mixer-settler and subsequently on the stage efficiency, purity and throughput of a mixer-settler plant. The effect of these two important hydrodynamic variables on the solvent extraction process will be discussed further in Section 1.5 and represents the central focus on mass transfer of this thesis.

1.3 Mass Transfer in Liquid-Liquid Dispersions

Mass transfer is a very important aspect in solvent extraction systems and poor mass transfer of a desired species from one phase to another would have a detrimental effect on the overall performance even if the chemical reaction kinetics were rapid. The overall extraction rate is a function of the both the chemical reaction rate and the mass transfer rate. The slower of the two would determine the maximum rate. The system can therefore be either mass transfer rate limiting or chemical reaction rate limiting. The chemical reaction rate is a function of temperature and concentrations of species, organic and aqueous and is usually fixed by extensive research programs. The aim is therefore to maximize the overall mass transfer rate, within limits, in order to minimize its effect on the overall extraction rate.

1.3.1 Mass Transfer Theories

A number of theories exit on mass transfer across liquid-liquid interfaces. These include the penetration theory, surface renewal theories and the two film theory (Perry and Green, 1999; Godfrey and Slater, 1994).

1.3.1.1 Penetration Theory

This theory proposes that as a freshly formed liquid surface (sphere) of one phase moves through the other phase, mass transfer decreases until it is mixed again at the next discontinuity. This theory allows for a random distribution of surface residence times.

According to the penetration theory, the liquid phase mass transfer coefficient is given by:

$$k_L = 2\sqrt{\frac{D_L}{\pi t}} \tag{1.6}$$

1.3.1.2 Surface Renewal Theories

These theories propose a mechanism of mass transfer involving the movement of eddies from the bulk of a fluid to the interface, followed by a short period at the interface during which time unsteady state molecular diffusion controlled by solute transfer takes place. Further eddies then arrive to displace fluid at the interface.

Surface renewal theory gives the liquid phase mass transfer coefficient as:

$$k_L = \sqrt{D_L\, s} \tag{1.7}$$

1.3.1.3 Two Film Theory

Whitman's two-film theory has long been used as a basis for measuring mass transfer coefficients and for designing equipment. If phase equilibrium has not been achieved and the reaction is fast compared with the rate of mass transfer, there would be two liquid films on either side of the interface between the phases which offer resistance to mass transfer. Thus, the reaction occurs as the solute diffuse through the films into the bulk of the other phase. This model assumes a steady state in which the local flux across each element of area is constant; i.e., there is no accumulation of the diffusing species within the film.

In film theory, the liquid phase mass transfer coefficient is given by:

$$k_L = \frac{D_L}{\delta} \tag{1.8}$$

Penetration theory is more difficult to use than film theory when the reaction process is very complex. The predictions or correlations based on the film model are often nearly identical to predictions based on the penetration and surface renewal models. Thus, in view of its relative simplicity, the film model is normally preferred for purposes of discussion or calculation (Perry and Green, 1999) and will be further discussed in the following section.

1.3.2 Mass Transport Across Interfaces

The following section explains the two film theory and its application to mass transport across a liquid-liquid interface. The section starts with the concept of flux across an interface and ends with

the methodology which was used to calculate the overall volumetric mass transfer coefficients in this thesis.

Mass transfer across an interface can be described in terms of a flux equation.

$$j = k_L \, \Delta C \tag{1.9}$$

where k_L is a mass transfer coefficient and ΔC is the concentration difference (driving force) between the bulk solution and the interface.

This concept is illustrated in Figure 1.10.

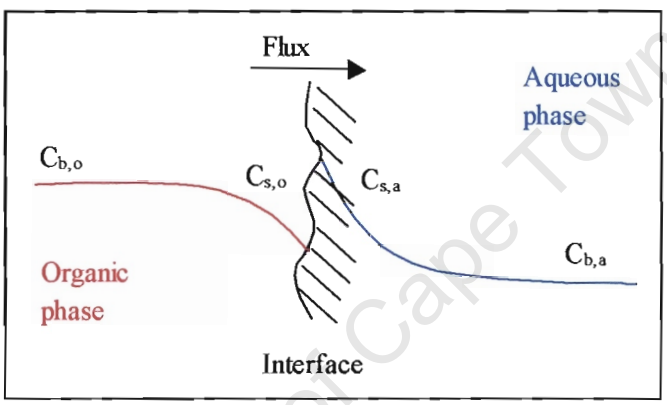

Figure 1-10 Illustration of the flux across a organic-aqueous interface (Nicol, 2004).

The flux across the liquid-liquid interface under steady state conditions can be written as (Nicol, 2004):

$$j = k_o \left(C_{b,o} - C_{s,o} \right) = k_a \left(C_{s,a} - C_{b,a} \right) \tag{1.10}$$

where k_o, k_a are mass transfer coefficients in each phase, $C_{b,o}$ is the concentration in the bulk organic phase, $C_{b,a}$ is the concentration in the bulk aqueous phase, $C_{s,o}$ is the concentration in the organic phase at the interface and $C_{s,a}$ is the concentration in the aqueous phase at the interface.

Equilibrium at the interface requires that:

$$C_{s,o} = D_c \, C_{s,a} \tag{1.11}$$

where D_c is the distribution coefficient of the desired species between the two phases. If we assume that $C_{s,o} >> C_{b,a}$, i.e. we start with no desired species in the aqueous phase, we can rearrange Equation 1.10 to give (Nicol, 2004):

$$j = \frac{k_a k_o D_c}{k_o D_c + k_a} C_{b,a} \tag{1.12}$$

and

$$K_L = \frac{k_a k_o D_c}{k_o D_c + k_a} \tag{1.13}$$

Equation 1.13 highlights the dependence of the overall mass transfer coefficient on the aqueous phase mass transfer coefficient, organic phase mass transfer coefficient as well as the distribution coefficient of the desired species.

The mass transfer rate equation for batch operation is as follows:

$$-\frac{dC}{dt} = K_L a \,(C_{org_{out}} - D_c \,.\, C_{aq_{out}}) \tag{1.14}$$

where K_La is the overall volumetric mass transfer coefficient and D_c is the distribution coefficient.

A similar approach can be followed for continuous operation. The mass transfer rate equation for continuous mixer-settler operation can be derived as follows:

$$Q_{aq} \,.\, C_{aq_{out}} = K_L a \,(C_{org_{out}} - D_c \,.\, C_{aq_{out}})\, V_{eff} \tag{1.15}$$

V_{eff} is an indication of the effective vessel volume, which is a function of macro-mixing and takes into account any dead zones. The overall mass transfer coefficient K_L is influenced by turbulent flow, the bulk flow shear and drop size. The interfacial area per unit volume parameter (a) is a function of the dispersion created and macro-mixing, which dictates phase hold-up and droplet sizes (Deglon, 2004).

The overall volumetric mass transfer coefficient (K_La) is a useful transport characteristic and is important in scale-up and equipment design. Transport characteristics depend on the physical

properties of the dispersion and on the equipment geometry and therefore the choice of impeller type is very important (Linek *et al*, 2002).

1.4 Dimensional Analysis

Dimensional analysis is central to the hydrodynamic study of mixer-settlers and is used in both the design and scale-up of such systems. The basis of dimensional analysis is such that similar fluid motion for different fluids or geometrical conditions can be compared.

An overview of dimensional analyses will be given in the following sections to clarify concepts that will be used later in Section 1.5.

1.4.1 Overview of Dimensional Analysis

One of the biggest problems faced when designing a plant based on laboratory scale results is the influence of variables on the scaled-up system. To circumvent this problem it is required to make use of a dimensional analyses technique, which will be discussed in this section. The basis of dimensional analysis is such that similar fluid motion for different fluids or geometrical conditions can be compared. This is possible if all variables describing a fluid system can be expressed in terms of the three fundamental units (mass, length and time). The number of variables in a mixing system can be restricted if only power requirements are considered. The remaining variables can be summarized into a number of main categories such as linear variables, fluid variables and dynamic variables (Rushton *et al*, 1950a; Rushton *et al*, 1950b).

1.4.1.1 Linear Variables

The main linear variables are listed in Table 1.1.

Table 1-1 Linear variables.

Variable	Meaning
T	Tank Diameter
D	Impeller Diameter
H	Liquid Depth
C	Impeller Height Above Tank Bottom

S	Pitch of the Impeller
L	Length of Impeller Blade
W	Width of Impeller Blade
J	Baffle Width
B	Number of Blades on Impeller
R	Number of Baffles

The variables in Table 1.1 are independent and systems can be designed where all the linear variables are a specific ratio of a dimension chosen as a reference. The dimensionless groups formed by the ratios of any of these variables to the reference dimension will have constant values. A system that is based on specific ratios to a reference dimension or dimensions is referred to as a geometrically similar system.

1.4.1.2 Fluid Variables

Table 1.2 summarizes the relevant fluid variables.

Table 1-2 Fluid variables.

Variable	Description
ρ_{org}	Organic Liquid Density
ρ_{aq}	Aqueous Liquid Density
μ_{org}	Organic Liquid Viscosity
μ_{aq}	Aqueous Liquid Viscosity

The variables such as average emulsion density and viscosity are functions of the variables listed above. Chemical concentrations for example, are taken into account by their effects on the variables summarized in Table 1.2.

1.4.1.3 Dynamic Variables

Table 1.3 summarizes the relevant dynamic variables.

Table 1-3 Dynamic variables.

Variable	Description
N	Impeller Speed
P	Net Power Input – Agitation power only
G	Gravitational Forces

From the above tables of linear, fluid and dynamic variables, it is clear that power (P) is the only dependent variable and is a function of the other variables.

1.4.2 Dimensionless Numbers

A series of important dimensionless numbers can be formed with the variables mentioned in Section 1.4.1. These numbers can and are frequently used for the designing and characterizing of mixing systems such as mixer-settlers.

Table 1-4 Dimensionless groups used in characterising mixer-settler mixing systems.

Dimensionless Group	Formula	Physical Meaning
Power Number (N_P)	$P/\rho_M N^3 D^5$	Ratio of actual to theoretical power consumption
Froude Number (N_{Fr})	$N^2 D/g$	Ratio of inertial to gravitational forces
Impeller Reynolds Number (N_{Re})	$\rho_M D^2 N/\mu_M$	Ratio of inertial to viscous forces
Flow Number (N_q)	$(Q_{aq}+Q_{org})/ND^3$	Combined flow rate to impeller pumping rate
Head Number (N_h)	$2gH/U_{tip}^2$ or $2gH/\pi^2 N^2 D^2$	Ratio of impeller head to tip speed

Post (2003) indicates that only three dimensionless numbers are needed to distinguish SX pumpers. These are the power number, the flow number and the head number. Together the three dimensionless numbers describe two characteristic plots: power-flow and head-flow. These plots are determined by experimentation. The advantage of these dimensionless plots is that they are valid for all sizes of geometrically similar pumpers and can be used to design and scale-up solvent extraction mixing systems.

The power number is well known in both the mineral and chemical engineering literature. The power number is considered to be an important scale-up criterion in the design of agitated vessels as it defines a critical ratio between the absorbed power and the theoretical power draw which should be independent of vessel size (Deglon *et al*, 2000). A higher power number indicates a higher power input, which results in a higher shear rate and an increase in overall mass transfer rate. Impellers of similar design but different sizes will have equal power numbers under dynamically equal conditions.

The Froude number is defined as the ratio between the centrifugal or inertial forces due to the pumping action of the impeller and the gravitational forces due to hydrostatic head in the agitated vessel. As a result, similar Froude numbers in different size vessels imply that hydrodynamic conditions between the two vessels are largely equivalent (Deglon *et al*, 2000). The dimensionless Froude number is used to describe the extent to which vortexing occurs and is a measure of the ratio of inertial stress, which is the flow of momentum created by bulk fluid motion and gravitational force per unit area acting on the fluid (Clemson University Website, 2004). The Froude number is used to correlate data at Reynolds numbers above 300 (Rushton *et al*, 2000b).

The Reynolds number is commonly used in fluid dynamics to determine the type of flow regime (whether laminar, turbulent or in transition between the two) in a pipe, where it is defined as $R_e = D.v.\rho_L/\mu_L$. In hydrodynamics, the impeller Reynolds number is the ratio of inertial forces, due to fluid flow, to the viscous forces. In agitated vessels, it is common to define the reference length as the impeller diameter and the reference velocity as revolutions per minute (of which tip speed is a function)

For the Reynolds number, the mean viscosity can be calculated as follows for unbaffled vessels (Perry 1999; Turnley 1970):

$$\mu_M = \frac{\mu_{aq}}{\phi_{aq}}\left(1+\frac{6\,\mu_{org}\,\phi_{org}}{\mu_{org}+\mu_{aq}}\right)\ ;\ \phi_{aq} > 0.4 \qquad (1.16)$$

$$\mu_M = \frac{\mu_{org}}{\phi_{org}}\left(1-\frac{1.5\,\mu_{aq}\,\phi_{aq}}{\mu_{org}+\mu_{aq}}\right)\ ;\ \phi_{aq} < 0.4 \qquad (1.17)$$

The mean density can be calculated as follows:

$$\rho_M = \rho_{org}\,\phi_{org} + \rho_{aq}\,\phi_{aq} \tag{1.18}$$

A number of additional hydrodynamic parameters can be formed using the variables mentioned in Section 1.4.1. These variables are summarized in Table 1.5

Table 1-5 Hydrodynamic properties.

Property	Formula
Power Intensity (kW/m^3)	P/V
Impeller tip speed (U_{tip}) (m/s)	πDN
Mean residence time	V/Q
Residence time distribution	RTD function

The power input per unit volume, or power intensity, is believed to be one of the more important parameters due to its effect on metallurgical performance and mixer-settler operating costs. Impeller tip speed is an important scale-up parameter, as it affects the velocity at which fluid leaves the impeller, and therefore affects dispersion and emulsion circulation (Deglon *et al*, 2000). The mean residence time and residence time distribution within the mixing vessel has a huge effect the overall stage efficiency.

1.5 Hydrodynamic Effects in Mixer-settler Mixers

This section is not a comprehensive overview of hydrodynamics, but focuses on hydrodynamic effects of relevance to this study i.e. the influence of impeller speed and type on mass transfer in a mixer-settler. The major sub processes occurring in mixer-settlers are hydrodynamics, organic-aqueous dispersion and phase disengagement (cf. Section 1.2.3). These sub processes all occur simultaneously in the mixing vessel and are strongly interdependent. However, organic-aqueous dispersion and phase disengagement are primarily affected by vessel hydrodynamics as this provides a suitable environment for each of these sub processes to occur. If the mixer vessel and impeller dimensions are fixed then hydrodynamics is primarily affected by the impeller speed, which strongly influences the power input to the mixing vessel. The following sections present an overview of the various hydrodynamic effects in mixer-settlers and the influence thereof on the parameters V_{eff}, a and K_L as was highlighted in Section 1.3.

1.5.1 Power Input

Power input is discussed in the following section under power intensity and power number. Power intensity is a function of impeller speed and type and is an indication of how much power is being put into the system. Power number is a function of impeller type and is an indication of how power is being put into the system.

1.5.1.1 Power Intensity

The power input to a mixer vessel defines the rate at which energy enters the vessel due to the action of the impeller. As the impeller turns it creates flow patterns within the vessel, where radial jets generated by the impeller strike the wall and separate into upper and lower wall jets, eventually dissipating the kinetic energy into heat. The power input reflects the rate at which energy is transferred to the fluid, which is the main driver for hydrodynamics in a mixing vessel. Power consumption is influenced as follows:

- Power consumption increases with increasing impeller diameter.
- Power consumption increases, with increasing impeller submergence.
- Power consumption increases with increasing the impeller speed.
- An increase in dispersion specific gravity results in a direct increase in power consumption.
- Tank dimensions have no influence on the power consumption for a given impeller profile. The clearance (the distance between the bottom of the tank and the impeller), though, has a marked effect on power consumption.

The power intensity (P/V) is defined as how much power is put into a specified volume of fluid and is the driving force for hydrodynamics, mixing and dispersion. From the literature it is evident that it is difficult to measure some of the individual variables such as the interfacial area per unit volume (a) in order to formulate models and therefore most researchers correlate the power intensity directly to the overall volumetric mass transfer coefficient (K_La) via empirical correlations.

Linek *et al* (2002) highlighted that the overall volumetric mass transfer coefficient (K_La) can be correlated to the power intensity (and gas superficial velocity) as follows:

$$K_L a = C_1 (e)^{C_2} v_s^{C_3} \tag{1.19}$$

where

$$e = e_{imp} + e_{gas} \tag{1.20}$$

and

$$e_{imp} = \frac{P}{V} \tag{1.21}$$

Equation 1.21 can be applied to solvent extraction systems, but without the gas velocity term, as follows:

$$K_L a = C_1 \left(\frac{P}{V}\right)^{C_2} \tag{1.22}$$

where C_1, C_2 are constants.

Moucha *et al* (2003) found the that the values of constant C_1 ranged from 1.13×10^{-3} to 2.86×10^{-4} and that the values of C2 ranged from 0.88 to 1.25 when a Na_2SO_4 solution was subjected to various multiple-impeller configurations.

Equation 1.22 shows that the higher the power input into the mixing vessel or power intensity, the higher the shear and therefore the higher the overall mass transfer rate when the constant C_2 is greater than 1.

Another useful parameter is the specific power input (ε), also known as the rate of energy dissipation, which is similar to the power intensity. Specific power input can be expressed in terms of fluctuating velocity (which reflects turbulence) and impeller diameter through a semi-empirical formula.

$$\varepsilon = C \frac{u'^3}{D} \tag{1.23}$$

Equation 1.23 shows that higher power intensities cause more turbulence which means better drop break-up and micro-mixing. Measurements of mean and fluctuating velocity can be carried out accurately by means of hot-wire, hot-film or Laser-Doppler anemometry.

The maximum energy dissipation rate can be calculated as follows (Pacek *et al*, 1999):

$$(\varepsilon_T)_{max} = (\varepsilon_T)_{imp} = \frac{P}{\rho_M V_{imp}} \quad (1.24)$$

Equation 1.24 highlights that the highest power intensity is in the impeller region which is relevant to droplet break-up as most break-up occurs in this region.

Sandler and Luckiewicz (1987) indicated that the typical power intensity for emulsification / dispersion is in the order of 5 – 9 kW/m^3.

1.5.1.2 Power Numbers

As discussed in Section 1.2.3, the power number defines a critical ratio between the absorbed power and the theoretical power draw which should be independent of vessel size for the same type of impeller. Different types of impellers generally have different power numbers and thus the power number is an indication of how the power is put into the vessel.

High power number radial flow impellers such as the Rushton turbine establishes high shear and turbulence in the impeller zone, high turbulence in the bulk vessel and induces medium pumping. The Rushton turbine is therefore well suited for drop break-up, drop coalescence and both micro-mixing and macro-mixing. These types of impellers give high overall mass transfer coefficients (K_L) as well as high interfacial area per unit volume (a) and good effective volumes (V_{eff}) for mass transfer. A Rushton turbine is illustrated in Figure 1.11.

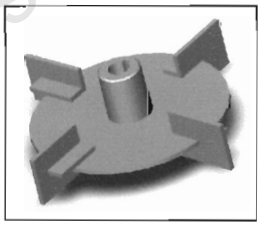

Figure 1-11 Illustration of a Rushton turbine (Post, 2003).

Moderate power number axial flow impellers such as the marine propeller generate low shear in the impeller zone and low turbulence in the bulk vessel. These types of impellers produce high pumping rates and although they do not produce small droplets or give good overall mass transfer coefficients (K_L) they are very good for bulk mixing. The interfacial area per unit volume (a) created by this type of impeller is also small due to low shear and low turbulence in the impeller zone as well as low turbulence in the bulk vessel. The overall mass transfer achievable with these

types of impellers is relatively poor. Axial flow impellers are better than radial flow impellers when high mixing intensity performance is required (Moucha *et al*, 2003). A Lightnin A110 propeller is illustrated in Figure 1.12.

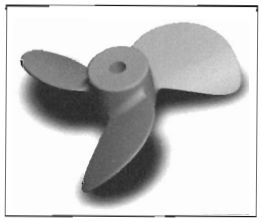

Figure 1-12 Illustration of a Lightnin A110 propeller (Post, 2003).

Low power number ultra high shear (UHS) impellers such as the spinning disc impeller establishes ultra high shear in the impeller zone, low turbulence in the bulk vessel and induces low pumping. The spinning disc impeller is therefore well suited for drop break-up, gives small droplets and low drop coalescence. These types of impellers give low overall mass transfer coefficients (K_L) due to low bulk flow and induced turbulence. They do on the other hand produce very high interfacial area per unit volume (a). Due to low pumping the macro-mixing is low and because of low turbulence the micro-mixing is also low resulting in poor effective volumes (V_{eff}) for mass transfer. Pacek *et al* (1999) found that low power number agitators of the high flow or ultra high shear type (Chemineer axial flow hydrofoil impeller – HE3, Chem Shear CS2 and CS4) produce much smaller drop sizes and narrower drop size distributions than "high shear", high power number agitators such as the standard Rushton turbine and the six-blade disc impeller at the same mean energy dissipation rates and do so more rapidly. The low power number impellers also achieve droplet size equilibrium more rapidly. Their findings highlighted that there are processing advantages to be gained for choosing a low N_P impeller when small drops of narrow size distributions are required.
A Chemineer Chemshear impeller is illustrated in Figure 1.13.

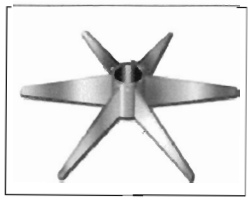

Figure 1-13 Illustration of a Chemineer Chemsheer impeller (Post, 2003).

Moderate power number radial flow impellers, which are intermediate in characteristics, fall between the Rushton turbine and the high speed spinning disc impellers. One of the designs is the

so-called pump mixer. The function of this impeller is to firstly pump fluid into the mixing vessel due to centrifugal forces exerted by the impeller blades on the liquid below the impeller, creating radial fluid jets and secondly to supply enough mixing to disperse the organic and aqueous phases enough for good mass transfer to occur. A Holmes and Navier and a curve bladed pumper is illustrated in Figure 1.14.

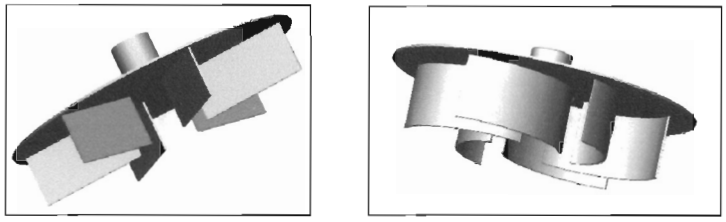

Figure 1-14 Illustration of a Holmes and Navier and a curve bladed pumper (Post, 2003).

In general, the high power number impellers such as the Rushton turbine gives the best overall volumetric mass transfer coefficients (K_La) due to the high overall mass transfer coefficients (K_L), high interfacial area per unit volume (a) and effective volumes (V_{eff}) for mass transfer achieved. A typical power number for a full-scale solvent extraction plant is 2.3.

1.5.2 Mixing

Mixing in mixer-settlers can be classified as macro-mixing or micro-mixing. Macro-mixing is related to the bulk mixing of fluids within the mixing vessel and micro-mixing refers to the micro phenomena caused by turbulence. Both macro-mixing and micro-mixing and their influence on mass transfer will be discussed in more detail in the following sections.

1.5.2.1 Macro-mixing

Macro-mixing refers to the bulk fluid flow within the mixer vessel and primarily affects the effective volume available for mass transfer (V_{eff}) as it ensures that all parts of the mixer vessel contains dispersed organic or aqueous. Improved macro-mixing generally increases mass transfer by increasing the effective volume available for mass transfer (V_{eff}) and can lead to higher interfacial areas for mass transfer.

Higher impeller speeds generally improve macro-mixing, especially for impellers with reasonable pumping rates, such as Rushton turbines or axial flow propellers. However, low pumping rate

impellers such as high speed spinning discs will not give good macro-mixing, even with increases in impeller speed.

1.5.2.2 Micro-mixing

Micro-mixing affects the overall mass transfer coefficient (K_L) and also affects the effective volume for mass transfer (V_{eff}). However, micro-mixing can reduce the effective interfacial area per unit volume (a) because it can increase drop coalescence within the mixing vessel. Ultra high shear impellers, which create small droplets with little turbulence, produce lower overall mass transfer coefficients (K_L) than Rushton turbines which create similar small droplets and high turbulence.

In the characterization of turbulence it is clear from Equation 1.23 that the power, and therefore impeller speed, has a large effect on the fluctuating velocity and, therefore, on the efficiency of micro-mixing in the mixing vessel. Hence, the impeller speed affects the power input to a mixing vessel, which in turn affects the level of micro-mixing.

1.5.3 Organic-Aqueous Dispersion

As discussed in Section 1.2.3, organic-aqueous dispersion refers to the ability to disperse the two phases in a manner conducive to enable mass transfer to take place between the two phases. Dispersion can be divided into two sub processes which include drop breakage and drop coalescence. Both these two opposing processes have an influence on the interfacial area per unit volume (a). Drop break-up increases the resulting interfacial area per unit volume (a) and drop coalescence reduces the interfacial area per unit volume. The degree of dispersion also affects the effective volume available for mass transfer (V_{eff})

Both the Rushton turbine type impellers and the spinning disc type impellers produce high interfacial area per unit volume (a), but the spinning disc creates less effective volume available for mass transfer (V_{eff}) than the Rushton turbine (i.e. macro-mixing is poorer). Based on this, the Rushton turbine should therefore facilitate better mass transfer. However, ultra high shear spinning disc impellers typically generate smaller droplets and therefore higher interfacial areas than Rushton turbines.

1.5.4 Scale-up

Scale-up is not the focus of this study, but in order to scale-down the full scale plant mixer-settler to a pilot plant scale mixer-settler it is important to understand the key variables and parameters that are influenced by the different plant sizes. Scaling therefore needs to be discussed in some detail, for two major reasons. Firstly, hydrodynamics is central to the scale-up of mixer-settlers and, secondly, the main objective of the experimental rig used for generating the results for this thesis is to assist in scale-up.

1.5.4.1 General Scale-up Criteria

Two main criteria exist when changing the scale of equipment with the goal of obtaining the same mixing performance at the new scale. These are:

- Geometric similarity should be preserved – dimensional ratios should be the same in the pilot plant unit as it is in the full-scale unit.
- Dynamic similarity should be preserved –Reynolds numbers should be the same in the pilot plant unit as it is in the full-scale unit.

Podgórska and Baldyga (2001) investigated the variance in drop size distributions in different sized agitated tanks based on various scale-up criteria. The criteria and major findings are listed below.

- Scale-up on equal power per unit volume (P/V) and geometrical similarity (D/T). The average circulation time (τ_c) increases on scale-up and larger drops are formed in larger scale systems due to domination of coalescence effects as a result of the increased residence time (τ) in the bulk. An increase in D/T decreases the difference between the drop size in the impeller and the bulk zone. An increase in power input per unit volume increases the difference between the drop size between the impeller and bulk zone.
- Scale-up on equal average circulation time (τ_c) and geometrical similarity (D/T). The power per unit volume increases with scale-up and much smaller drops in larger tanks are formed. The difference in the drop size between the impeller and the bulk zone increases when scaling- up.
- Scale-up on equal power per unit volume (P/V), equal average circulation time (τ_c) and no geometrical similarity (D/T). This results in a rather small increase in drop size when scaling up and a small difference in the drop size between the impeller and the bulk zone.
- Scale-up on equal impeller tip speed (ND) and geometrical similarity (D/T). Scaling up varies both the power input (P/V) as the average circulation time (τ_c). This results in a

significant growth in drop size when scaling up due to the combined effects of increased circulation time (τ_c) and decreased power per unit volume (P/V).

Based on the above findings by Podgórska and Baldyga it is clear that considerable thought should go into the process of selecting a scale-up criteria to ensure that the required drop size obtained is not only conducive to mass transfer, but also large enough for coalescence to take place within the settler residence time.

When scaling up or down, turbulence should be induced to entrain slow moving parts within faster moving parts. Turbulence is the highest near the impeller and liquid should be circulated through this region as much as possible. A vortex should be avoided because adjoining layers of circulating liquids travel at similar speed and entrainment does not take place – the liquids simply rotate around the impeller (Young, 2001).

1.5.4.1.1 Geometric Scale-up

Geometric scale-up implies that the pilot plant and the full-scale operation should be geometrically similar, in other words, the one should look exactly the same as the other except for size. Sandler and Luckiewicz (1987) highlighted the following parameters to be considered when specifying agitators:

- Impeller diameter
- Impeller revolutions per minute
- Impeller type
- Vessel volume
- Vessel geometry
- Agitator location with reference to the vessel
- Vessel internals – baffles etc.

1.5.4.1.2 Hydrodynamic Scale-up

The starting point of hydrodynamic scale-up is geometrical scale-up. For hydrodynamic scale-up to apply, geometrical similarity between laboratory and full-scale mixer vessels should apply. Hydrodynamic scale-up takes geometrical similarity further by attempting to reproduce the hydrodynamic conditions that exist within the laboratory mixing vessel in the industrial size version. This rests on the premise that, if certain hydrodynamic conditions produce a certain

metallurgical result in a laboratory test, then those same conditions will produce the same metallurgical result in a full-scale mixer-settler.

Hydrodynamic scale-up makes use of a number of dimensionless groups. The most important of these groups are the power number, the impeller Reynolds number and the Froude number as highlighted in Section 1.4.2. Another criteria frequently being used when scaling up mixer-settlers is constant tip speed.

It is clear then that hydrodynamic scale-up is largely based on ensuring that the ratio of actual to theoretical power consumption remains constant, that the ratio of inertial to gravitational forces are the same and also to ensure that the ratio of inertial to viscous forces are comparable on both pilot and full scale plant operations.

1.6 Influence of Impeller Speed and Type on Overall Mass Transfer

The following section highlights the influence of impeller speed and type on the overall mass transfer of species from one phase to another in liquid-liquid extraction. Both the impeller design and its rotational speed have an influence on the mixer-settler hydrodynamics and therefore the overall volumetric mass transfer coefficients.

1.6.1 Impeller Speed

An increase in impeller speed (N) results in an increase in impeller power (P) according to Equation 2.1 and therefore will also result in an increase in the power per unit volume (P/V). It is this power intensity or power per unit volume that causes turbulence within the mixer vessel. Higher power intensities result in higher turbulence and therefore better micro-mixing. The increase in micro-mixing results in an increase in the mass transfer coefficient (K_L). An increase in impeller speeds results in higher shear and turbulence in the impeller zone which results in an increase in drop break-up and an increase in the interfacial area per unit volume (a) and therefore the overall volumetric mass transfer coefficient (K_La). An increase in the impeller speed also increases macro-mixing, which improves the effective volume (V_{eff}) for mass transfer.

1.6.2 Impeller Type

Different impellers have different shear, turbulence and pumping characteristics which affects the mass transfer of species between organic and aqueous phases.

High power number radial flow impellers such as the Rushton turbine establishes high shear and turbulence in the impeller zone, high turbulence in the bulk vessel and induces medium pumping. It is therefore well suited for drop break-up, drop coalescence, both micro-mixing and macro-mixing and gives high mass transfer coefficients (K_L) as well as high effective volumes (V_{eff}) for mass transfer. This type of impeller can therefore give good overall volumetric mass transfer coefficients (K_La).

Moderate power number axial flow impellers such as marine propellers generate low shear in the impeller zone and low turbulence in the bulk vessel. This type of impeller produces high pumping rates and does not give good mass transfer coefficients (K_L). The interfacial area per unit volume (a) created by this type of impeller is also small due to low shear and low turbulence in the impeller zone as well as low turbulence in the bulk vessel. The mass transfer achievable with these types of impellers is relatively poor.

Low power number ultra high shear (UHS) impellers such as the spinning disc impeller give low mass transfer coefficients (K_L) due to low bulk flow and induced turbulence. They do on the other hand produce very high interfacial area per unit volume (a). Due to low pumping the macro-mixing is low and because of low turbulence the micro-mixing is also low resulting in poor effective volumes (V_{eff}) for mass transfer. UHS impellers can therefore give reasonably good overall volumetric mass transfer coefficients (K_La).

Moderate power number radial flow impellers such as being used in the solvent extraction industry and PMR have intermediate characteristics between the Rushton turbine and the high speed spinning disc type impellers

1.7 Scope of Thesis

From the reviews presented in this chapter it should be clear that mixer-settler hydrodynamics, driven by the central hydrodynamic variables of impeller speed and type has profound effects on mixing in a mixer-settler. However, comparatively little work has been performed on quantifying the effect of these variables in stripping of palladium from a typical palladium organic. It is believed, therefore, that it is important to obtain a better understanding of the way in which power

input, as influenced by impeller speed and type, affects the kinetics of the palladium stripping reaction.

The aim of this thesis is to categorize the effect of hydrochloric acid normality and temperature on the thermodynamics of the palladium stripping reaction and secondly to determine the effect of impeller speed and type on the kinetics of the stripping of palladium from a typically loaded palladium organic. The thesis explores the effects of impeller speed and type on hydrodynamics, palladium stripping rates and overall volumetric mass transfer coefficients. The study was carried out using a 1/5-scale palladium mixer-settler pilot plant manufactured at the Anglo Platinum Research Centre using typical plant feed and palladium organic.

2 Experimental

This chapter presents details of the experimental program and equipment used for the study on palladium stripping kinetics and the mass transfer of palladium from a typical palladium loaded organic to the stripping acid. Section 2.1 describes the feed preparation, which includes organic make-up, palladium feed solution preparation, loaded palladium organic preparation and strip acid preparation. Section 2.2 deals with sample analyses and Section 2.3 covers the palladium stripping characterization experimental program, which includes the experimental design, equipment as well as the experimental set-up. Section 2.4 covers the influence of impeller speed and type on the hydrodynamics and therefore the mass transfer of the palladium stripping reaction.

2.1 Feed Preparation

In order to eliminate as much of the experimental variability associated with the feed variability, feed preparation was necessary to generate enough homogenous feed for the whole of the experimental program. The feed preparation done for the experimental program is discussed in the following sections.

2.1.1 Organic Make-up

The palladium organic was made-up using the supplied constituents as being used by the Anglo Platinum PMR refinery. It was decided against the use of previously made-up plant organic, since contamination and organic degradation would impact significantly on the results obtained. The palladium extractant was mixed together with the diluent and catalyst was added according to the standard PMR industrial procedures using the following method. The density of each of the constituents was determined using an Anton Paar DMA 5000 density meter. From the acquired densities, the required constituent volumes were converted to mass and the required mass of each of the constituents was weighed on a Sartorius Genius ME415S laboratory balance before being mixed together. A sample from the "fresh" bulk palladium organic was taken, loaded to its maximum capacity with copper and was analyzed for the palladium extractant to verify it's concentration in the bulk organic. A Titralab 900 titration system was used for the analyses by titrating with 3N NaOH and calculating the palladium extractant concentration by means of an H^+ mass balance.

2.1.2 Pd Feed Solution Preparation

The palladium feed solution as received from the PMR plant was filtered through Whatman 540 filter paper in order to remove any post precipitated PGM and base metals. The filtered feed was sampled and analyzed in duplicate for PGM and base metals using a Spectro Ciros ICP.

2.1.3 Loaded Palladium Organic Preparation

To be able to do the stripping experiments, the "fresh" bulk organic had to be loaded with palladium to a predetermined concentration, thereby mimicking the extraction section of the PMR palladium solvent extraction plant. The "fresh" bulk palladium organic was contacted with filtered palladium feed solution using a Heidolph R2020 overhead stirrer for two hours. This extended contact period may not have been necessary, but ensured extraction to the equilibrium. The organic and aqueous was phase separated using separation funnels and the organic phase was filtered through Whatman PS1 filter paper to trap any entrained aqueous solution. The loaded organic was sampled and the sample stripped with 32% HCl using five contacts. The loaded strip acid was analyzed for palladium using a Spectro Ciros ICP and the result was used to calculate the palladium concentration in the bulk loaded organic by means of a mass balance.

A second loaded organic sample was taken, prepared using glacial acetic acid and analyzed for palladium content using a Varian Vista-Pro ICP-OES. The palladium in the loaded organic analyses from the Varian ICP was compared to the mass balanced result from the Specto Ciros ICP. The concentration of Pd in the loaded organic was also determined by mass balance from the bulk palladium feed concentration and aqueous and organic volumes.

The two palladium ICP analyses using the methods described above corresponded to within 97% of the mass balance and therefore indicated a high degree of accuracy on the methods used and also both the accuracy of the Spectro Ciros and Varian ICPs. This loaded organic containing 11.7 g/l palladium forms the basis of all the subsequent experiments.

2.1.4 Strip Acid Preparation

Strip acids were prepared at five different HCl concentrations for all the subsequent experiments using Merck 32% HCl and ultra pure water for dilution purposes. The required HCl concentrations were 4N, 4.5N, 5N, 5.5N as well as 6N. The concentrations of each of the acids were determined using an Anton Paar DMA 5000 density meter since a direct correlation exists between acid

strength and density. Table 2.1 summarizes the relationship between HCl concentration and density.

Table 2-1 Acid normalitiy and corresponding density.

[HCl]	Density g/cm^3
6N	1.09787
5.5N	1.09006
5N	1.08215
4.5N	1.07415
4N	1.06606

The prepared strip acid normalities were checked using a Titralab 900 titration system by titrating with 3N NaOH.

2.2 Sample Analyses

All samples taken during the test work were analyzed at the Anglo Platinum Research Centre's Process Research Laboratories using a variety of laboratory equipment. The results obtained were verified by duplicate analyses and rigorous instrument calibration, diagnostics and drift standards.

2.2.1 PGM and Base Metal Analyses

All the PGM and base metal analyses were done using either the Specto Ciros ICP or the Varian Vista-Pro ICP-OES. Throughout the experimental program, the ICP diagnostics program was run to verify that the instrument was operating correctly before each set of samples was analyzed. The ICP was also calibrated using eight standards (four PGM, one base metal, one amphoteric, one blank and one drift standard) before analyzing samples and a drift standard was read after every ten samples to detect any instrument drift.

All the samples were diluted with 3N HCl using a Microlab 500 series auto diluter before being subjected to ICP analyses. Scandium was used as the reference element since scandium is not prevalent in the samples being analyzed.

2.2.2 Density Analyses

The density of samples was measured in triplicate using an Anton Paar DMA 5000 density meter which was calibrated against ultra pure water with a density of 0.99820 ± 0.00001 g/cm^3 at 25°C. Both organic and aqueous samples were analyzed using the same instrument, but after every sample the instrument reading was checked with ultra pure water and if any drift was noted the instrument was rinsed with copious amounts of ethanol, ultra pure water and was dried by blowing air through the instrument before recalibration.

2.2.3 Normality Analyses

The normality of samples was analysed using a Titralab 900 titration system by titrating with 3N NaOH. All samples were analyzed in duplicate.

2.2.4 Tracer Analyses

All samples taken during the residence time distribution test work were subjected to a Varian Cary 50 UV-vis spectrometer for concentration analyses. The wavelength used was 515 nm which corresponds well with the red dye (Moir's red food colourant) used for the concentration profiles.

2.3 Palladium Stripping Characterization

This section presents the experimental procedure and experiments done to determine the palladium stripping rate by varying two process variables, namely temperature and strip acid (HCl) concentration. It must be noted that other variables such as palladium concentration and palladium organic extractant concentration also influences the thermodynamics, but these fall outside the scope of this study and requires a more fundamental research effort. A set of optimal operating conditions based on the findings of this test work was used in subsequent test work to determine the influence of impeller speed and type on hydrodynamics and mass transfer coefficients.

2.3.1 Experimental

The purpose of this experimental program was to characterize the palladium stripping reaction rate in terms of different operating temperatures and stripping acid concentrations. Due to accelerated organic degradation at elevated temperatures, the maximum operating temperature was limited to

40°C. The strip acid normality range was kept between 4.0 N and 6.0 N based on plant experience. The experimental conditions are summarized in Table 2.2.

Table 2-2 Experimental conditions.

[HCl] / T	Temp 1	Temp 2	Temp 3
N 1	6N, 35°C	6N, 25°C	6N, 15°C
N 2	5.5N, 35°C	5.5N, 25°C	5.5N, 15°C
N 3	5N, 35°C	5N, 25°C	5N, 15°C
N 4	4.5N, 35°C	4.5N, 25°C	4.5N, 15°C
N 5	4N, 35°C	4N, 25°C	4N, 15°C

The experimental setup consisted of a 60mm x 60mm x 100mm Perspex mixing vessel (unit cell) inserted into a water bath. A Heidolph R2020 (0-1800 RPM) overhead stirrer fitted with a titanium 4-bladed turbine was used to generate the liquid-liquid dispersion needed for the distribution of palladium species between the organic and aqueous phases. The experimental setup is illustrated in Figure 2.1. The water bath temperature was controlled by a Selecta Frigiterm water controller at the desired experimental temperature. The water temperature controller is illustrated in Figure 2.2.

Figure 2-1 Experimental setup.

Figure 2-2 Selecta Frigiterm water controller.

A scouting experiment was done with 6N HCl at 25°C to determine the reaction rate. This rate then dictated the sampling frequency to be used in the fifteen experiments in order to get enough samples spread out over the reaction time under review.

Depending on the temperature at which an experiment was to be performed, the Selecta Frigiterm water controller temperature was set higher than 15, 25 or 35 °C to cater for heat losses to the environment. The water bath was run for at least an hour and the water temperature checked with a thermometer before the start of an experiment to verify that the water temperature was at steady state.

The loaded organic as well as the strip acid were placed in another water bath to preheat both the loaded organic and aqueous feed to the desired experimental temperature. The Perspex mixing vessel was placed in the water bath and the 4-bladed turbine fitted to the overhead stirrer by aligning it to approximately 3mm from the bottom of the mixing vessel. The stirrer was started to check for alignment and switched off. The preheated organic (155ml) was then added to the mixing vessel and the agitator started and run at 100 RPM. After 10 minutes a thermometer was used to check that the organic was at the required experimental temperature before the agitator speed was adjusted to 1600 RPM, the strip acid (45ml) was added and sampling commenced.

Sampling of the dispersion in the mixing vessel was done at 1, 2, 3, 4, 5, 10 and 30-minute intervals. If the reaction was slow according to visual inspection of the strip acid colour, sample taking was extended to 40, 50 and even 60 minutes to complete the profiles. The samples (10 ml) were phase separated using phase separation funnels. The aqueous fractions were then filtered through Whatman 540 filter papers to remove any entrained organic. The filtered aqueous fraction was then analyzed for PGM and base metals using the Spectro Ciros ICP.

Equilibrium experiments were done by contacting different volumes of loaded organic with 6N strip acid in separation funnels for four hours using a Labcon shaker. The organic and aqueous phases were then phase separated and filtered through Whatman PS1 and Whatman 540 filter paper respectively. The organic and aqueous fractions were then analyzed by ICP.

2.4 Hydrodynamic Characterization

This section presents the experimental procedure and experiments done to determine the influence of impeller speed and type on the hydrodynamics and therefore the overall palladium stripping rate. A set of operating conditions (6N HCl and 25°C) based on the findings of test work in Section 2.3 was used throughout this test work program.

2.4.1 Experimental

The purpose of this experimental program was to determine the influence of different impeller speeds and types on the hydrodynamics as well as the stripping rate of palladium from a typically loaded palladium organic in a mixer-settler. The experiments were done at 25°C using 6N HCl as the stripping medium. These conditions were chosen based on the results and discussion in Section 3.1.2.

In Section 1.5.1.2 the three types of impellers (high N_p Rushton turbine, moderate N_p propeller and low N_p spinning disc) were discussed to illustrate the extremes of expected behaviour for different impellers. Only the Rushton turbine and a 4-bladed radial disc impeller were selected for the experiments used in this study because of their common application in the solvent extraction and mixing industries. The Ruston turbine was selected because it gives high mass transfer coefficients (K_L) as well as high interfacial area per unit volume (a) and the 4-bladed radial disc impeller was selected because it is a solvent extraction pump-mix standard which has intermediate characteristics between a Rushton turbine and a high speed spinning disc impeller as a result of the disc and the low height blade design.

A propeller was not chosen as it is poor for dispersion generation and gives poor mass transfer coefficients. A high speed spinning disc was also not chosen because although it generates very high interfacial area per unit volume (a), it does not give a very high mass transfer coefficient (K_L) and more pertinently, the small droplets generated could result in coalescence problems in the settler due to stable emulsion formation.

A 1/5 scale Perspex mixer-settler was manufactured based on the stripping mixer-settler design drawings from the operating plant. A 1/5 scale "PMR" 4-bladed radial disc impeller as well as a 6-bladed Rushton turbine was also manufactured. The 1/5 scale mixer-settler is illustrated in Figure 2.3 and the Figure 2.4 illustrates the 1/5 scale "PMR" 4-bladed radial disc impeller as well as a 6-bladed Rushton turbine.

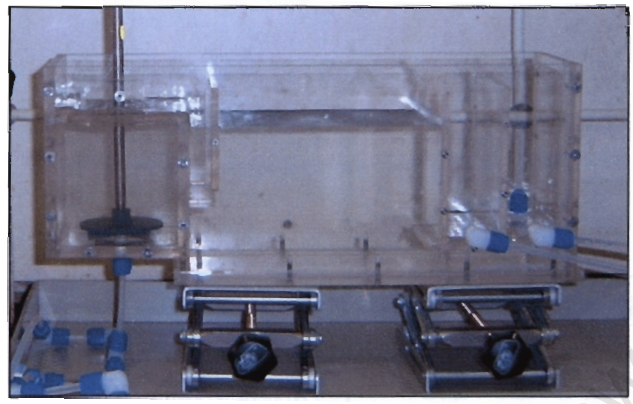

Figure 2-3 1/5 scale Perspex pilot plant mixer-settler.

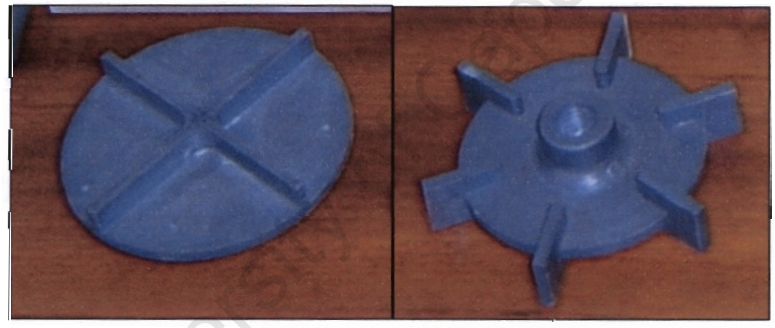

Figure 2-4 4-bladed radial disc impeller as well as a 6-bladed Rushton turbine.

The feed rate of both the organic and aqueous phases to the pilot plant mixer-settler used for all the experiments was controlled using two Masterflex positive displacement pumps. The required flow rates were obtained using Masterflex modular controllers and the flow rates were calibrated using 50ml and 100 ml volumetric flasks and monitoring the time required to fill them. The controllers were then fine tuned to give the required flow rates of loaded organic as well as strip acid. Figure 2.5 and Figure 2.6 illustrates the Masterflex pumps and modular controllers used for the required flow rates.

Figure 2-5 Masterflex metering pumps.

Figure 2-6 Masterflex modular controllers.

The power draw by the impeller motor cannot be used for the power intensity calculations since the it must be noted that the value of P is that exerted on the impeller shaft and not that of the motor driving the impeller due to motor inefficiencies. To be able to determine the power exerted on the shaft, a correlation between torque and RPM can be used.

$$Power = 2\,\pi\,N\,Torque \tag{2.1}$$

The torque can be measured using a dynamometer and rotational speed using a tachometer (Rushton *et al*, 1950a).

A Heidolph R2020 laboratory overhead stirrer was used for all the experiments and the stirrer was modified to enable the determination of torque exerted onto the impeller. This was done by removing the retort stand connection that comes standard with the stirrer. The stirrer was mounted onto a bearing enabling the stirrer to turn "freely" around the impeller shaft axis. A grooved disc was attached to the overhead stirrer and a string was attached to the disc and was inserted into the groove. The other end of the string was connected to a reference weight that was placed on a Sartorius balance. Any movement by the "free" running overhead stirrer could therefore be detected by noting the difference in the reading of the balance due to a decrease in the measured weight as a result of the overhead stirrer pulling on the string that is connected to the reference weight. From this weight difference the impeller torque could be calculated using Equation 2.1. Figure 2.7 illustrates the Heidolph R2020 overhead stirrer and Sartorius laboratory balance setup.

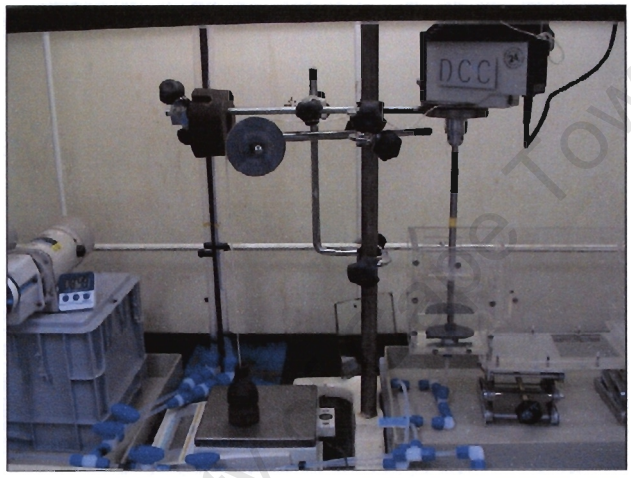

Figure 2-7 Modified Heidolph R2020 overhead stirrer and Sartorius balance setup.

The complete experimental setup highlighting the 1/5 scale mixer-settler, modified overhead stirrer, balance, pumps and controllers is illustrated in Figure 2.8.

Figure 2-8 Experimental setup for hydrodynamic characterization experiments.

All the experiments were done under equivalent conditions and these are tabled in Table 2.3 below.

Table 2-3 Standard experimental conditions.

Condition	Value	Units
Organic flow rate	2.69	l/hr
Aqueous flow rate	0.78	l/hr
Temperature	25	°C
Strip Acid (HCl)	6	N

The first set of experiments was done using a 4-bladed radial disc impeller and increasing the impeller rotational speed from 900 to 1300 RPM using increments of 100 RPM per individual experiment. This corresponds to an 11.1% increase in tip speed per experiment based on the tip speed at 900 RPM. The full scale plant impellers run at 200 RPM, which is equivalent to 1000 RPM on the pilot plant. The experimental matrix is summarized in Table 2.4.

Table 2-4 Experimental matrix for 4-bladed radial disc impeller.

Experiment number	4-bladed radial disc turbine (RPM)
1	900
2	1000
3	1100
4	1200
5	1300

The second set of experiments was done using a Rushton turbine with the same dimensions as the scaled down 4-bladed radial disc impeller. The experimental rotational speeds were varied from 790 to 1040 RPM to approximate the same power per unit volume as was obtained by the 4-bladed radial disc impeller. The required rotational speeds for the Rushton turbine was determined on the basis of adjusting the RPM, measuring the resulting torque exerted on the impeller shaft and calculating the resultant power per unit volume (P/V). An iterative process was followed by changing the impeller shaft RPM until the calculated P/V of the Rushton turbine corresponded to

that of the corresponding 4-bladed radial disc impeller experiment. The experimental matrix is summarized in Table 2.5.

Table 2-5 Experimental matrix for Rushton turbine.

Experiment number	Rushton turbine (RPM)
1	≈ 790
2	≈ 830
3	≈ 910
4	≈ 970
5	≈ 1040

Each experiment was run for 90 minutes (4x mean mixer vessel residence times) before a 20 ml sample of the dispersion was taken from the mixer vessel. This sample was phase separated using phase separation funnels. Each fraction was filtered through Whatman PS1 and Whatman 540 filter paper respectively to remove any entrainment. The organic and aqueous fractions were then analyzed by ICP.

The data recorded during the experiments can be seen in Appendix B.

3 Results and Discussion

The results presented in this chapter are derived from and are applicable to the experimental program outlined in chapter 2. Palladium stripping characterization results are presented in Sections 3.1 and hydrodynamic characterization and mass transfer results are presented in Section 3.2. The data and calculations for this charter are attached in Appendix A and B.

3.1 Palladium Stripping Characterization

This section presents the data obtained from the palladium stripping characterization experiments as outlined in Section 2.3. The results of the stripping kinetics experiments and the palladium stripping isotherm are presented in Section 3.1.1 and 3.1.2 respectively. The results for the fifteen batch palladium stripping characterization experiments are presented in Appendix A and are summarized in Figure 3.1. The palladium stripping equilibrium isotherm for 6N strip acid at 25°C is presented in Section 3.1.3 and a McCabe-Thiele construction at the same conditions is presented in Section 3.1.4.

3.1.1 Stripping Kinetics Experiments

Figure 3.1 is a graph of palladium concentration in the aqueous phase versus time and is based on the results obtained from contacting fifteen batches of loaded organic with strip acid at various normalities and temperatures.

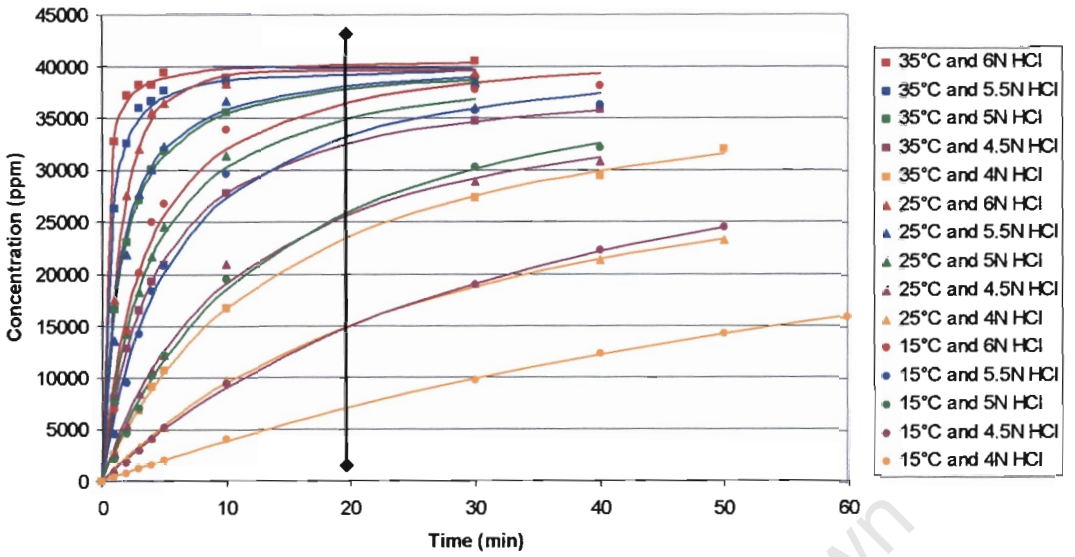

Figure 3-1 Strip acid concentration vs. time (O:A – 3.5:1).

From Figure 3.1 it is evident that the palladium stripping rate increases as the temperature increases and also with an increase in strip acid concentration. The average plant stripping mixer vessel residence time is approximately 20 minutes at the 100l/hr strip acid flow rate (see vertical line) which highlights the requirement for a stripping rate that is sufficiently fast in order for the process to be done in the operating plant counter current mixer-settlers. The stripping rates of all the experiments done at 4N, the experiments done at 4,5N and low temperatures as well as the experiment done at 5N and 15°C are too slow to be implemented, since it would require additional mixer-settlers to achieve the required separations.

From these results it is evident that the palladium stripping reaction rate is relatively fast at the higher temperatures and strip acid normalities. It must be noted that these reaction rates were done under conditions with no mass transfer limitations due to the 4-bladed turbine being run at 1600 RPM.

3.1.2 Stripping Isotherms

Based on the observations in Section 3.1.1 and taking into account organic degradation at high acid strengths and high temperatures the best operating strip acid normality would be somewhere

between 5.5N and 6N HCl at temperatures above 25°C and not exceeding 40°C. Figure 3.2 highlights the percentage stripping achievable at various temperatures and strip acid strengths within a twenty minute mixer vessel residence time.

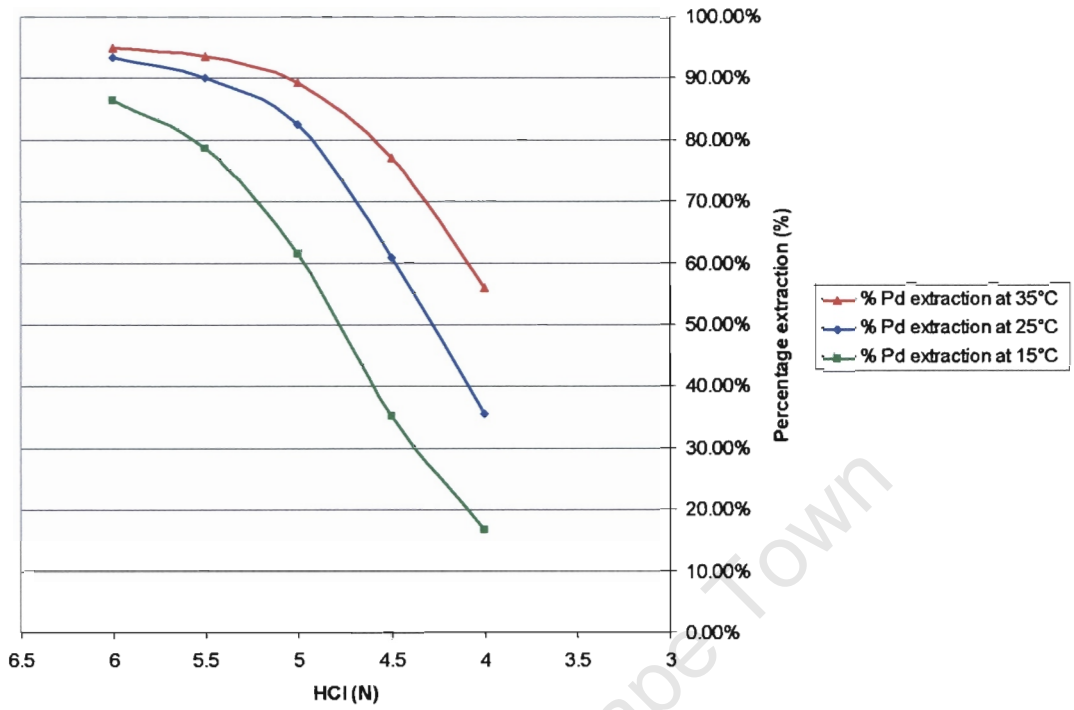

Figure 3-2 Percentage Pd extraction as a function of temperature and strip acid normality at 20 minutes mixer vessel residence time.

Again it should be noted that stripping with >5N HCl is adequate at temperatures above 25°C, but the percentage stripping achievable in a mixer-settler becomes very low at temperatures below 25°C.

From Figure 3.2 it is evident that the difference in extraction achievable with 6N HCl strip acid at 25°C and 35°C is negligible. All the subsequent experiments were done with 6N HCl at 25°C due to the reactions being fast enough to ensure that the real system will be mass transfer limiting. It is also unnecessary to have high reaction rates at conditions which damage organic and are a safety hazard while the real system is mass transfer limiting.

3.1.3 Stripping Equilibrium Isotherm (6N HCl, 25°C)

The next step in characterizing the palladium stripping reaction at 25°C and 6N strip acid normality is to construct a palladium stripping equilibrium isotherm, from which a McCabe-Thiele

construction can be done to evaluate the required number of counter current palladium stripping mixer-settlers. The equilibrium experimental data are presented in Appendix A. Figure 3.3 indicates the relationship between the palladium concentrations in the aqueous and organic phases.

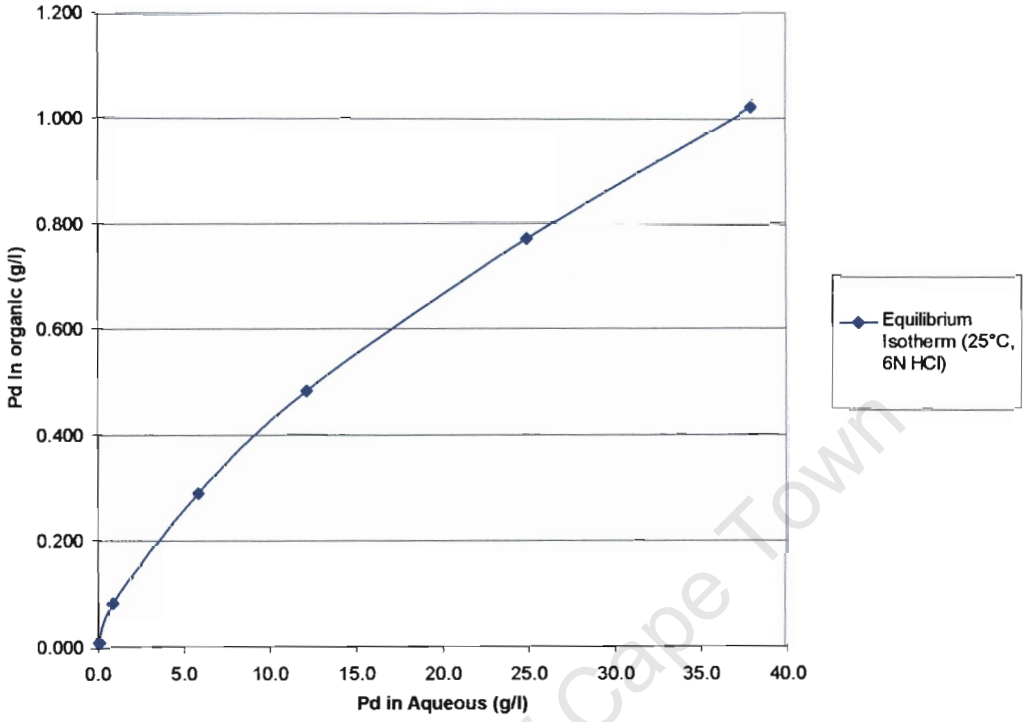

Figure 3-3 Pd stripping equilibrium isotherm (25°C, 6N HCl).

It should be noted that the distribution coefficient is not constant and the equilibrium line can be approximated by a function of the form: $Y = a X^{b}$. The data was fitted using DataFit version 8.0 software from Oakdale Engineering and the function is as follows:

$$Pd_{org} = 0.0876 Pd_{aq}^{0.677}, \qquad R^2 = 0.9993 \tag{3.1}$$

and $D_c = [Pd]_{org} / [Pd]_{aq}$ where D_c varies between 0.027 and 0.081

3.1.4 Stripping McCabe-Thiele Construction

The equilibrium data as highlighted in Section 3.1.3 can be used to construct a McCabe-Thiele construction to determine the minimum number of counter current stages that would be needed

under ideal conditions (100% stage efficiency) to strip palladium from the loaded organic leaving very low concentrations in the final stripped organic.

Figure 3.4 and Figure 3.5 illustrates such McCabe-Thiele constructions highlighting the required seven ideal stages. Figure 3.5 is a zoomed section of the region of the origin in Figure 3.4.

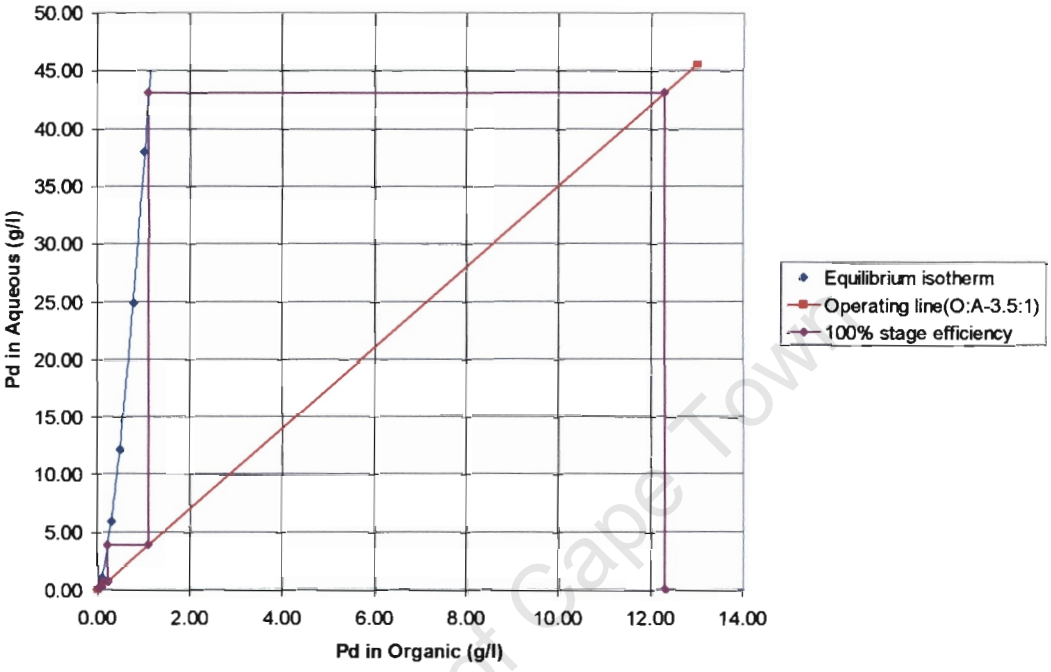

Figure 3-4 McCabe-Thiele construction (Ideal at 100% stage efficiency).

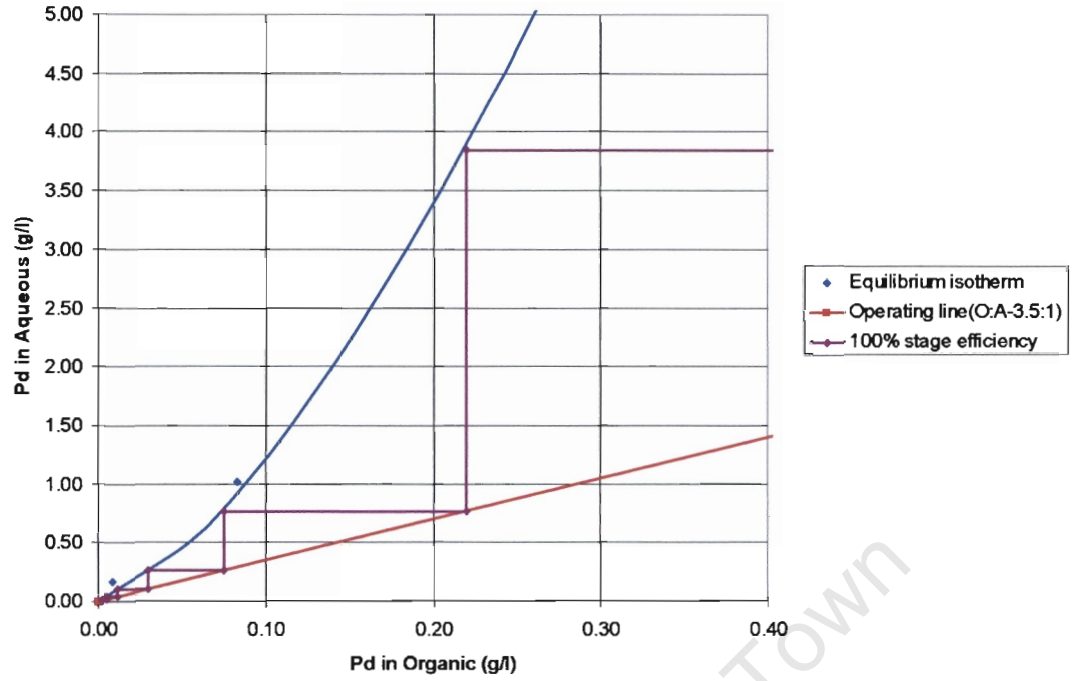

Figure 3-5 McCabe-Thiele construction at low concentrations (Ideal at 100% stage efficiency).

From Figures 3.4 and 3.5 it is clear that the operating line and the equilibrium line are very close to each other below a palladium in organic concentration of 0.1 g/l and this necessitates a large number of mixer-settlers to get to low concentrations within the organic phase. This problem can be alleviated by decreasing the O:A ratio to approximately 2.5:1. By doing this, the residence time in the mixers would increase, allowing more time to reach stage equilibrium, but the overall plant throughput would decrease and the need to further concentrate the strip acid by means of evaporation processes downstream would increase.

3.2 Hydrodynamic Characterization

The results presented in this section are derived from and are applicable to the experimental program outlined in Section 2.4. Section 3.2.1 covers power input and power intensity whilst mixing is covered in Section 3.2.2. Section 3.2.3 deals with mass transfer and the stripping of palladium as a function of impeller speed. The experimental data and calculations for this section are attached in Appendix B.

3.2.1 Power Input

The first set of experiments was done using a 4-bladed radial disc impeller at various impeller rotational speeds. The impeller speeds was varied between 900 to 1300 RPM using increments of 100 RPM per individual experiment. Figure 3.6 illustrates the tip speed and power intensity as a function of impeller rotational speed.

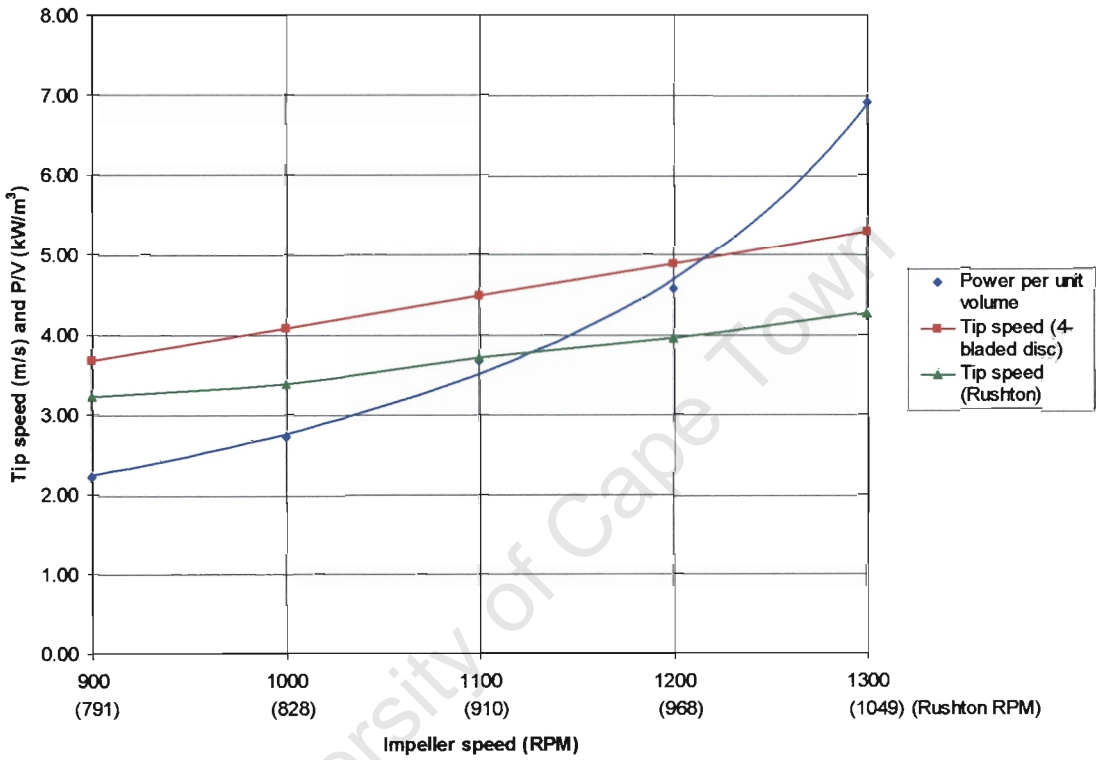

Figure 3-6 Power intensity and tip speed as a function of impeller RPM.

From Figure 3.6 it is clear that the power intensity of both the 4-bladed radial disc impeller and the Rushton turbine increases with an increase in impeller speed. The Rushton turbine has a lower tip speed than the 4-bladed radial disc impeller at equivalent power intensities. It can be seen from Table 3.1 that the power per unit volume of the 4-bladed radial disc impeller at 1000 RPM is approximately 2.7 kW/m^3 based on an effective mixer vessel volume of 1.24 liter.

Table 3-1 Power Input for the 4-bladed radial disc impeller.

Impeller speed (RPM)	N (s^{-1})	D(m)	Power (W)	Dispersion Density (kg/m3)	P/V (kW/m^3)	Np
900	15.0	0.078	2.762	933.7	2.23	0.304
1000	16.7	0.078	3.376	933.7	2.72	0.271
1100	18.3	0.078	4.558	933.7	3.68	0.274
1200	20.0	0.078	5.525	933.7	4.57	0.256
1300	21.7	0.078	7.581	933.7	6.94	0.277

Table 3-2 Power Input for the Rushton turbine.

Impeller speed (RPM)	N (s^{-1})	D(m)	Power (W)	Dispersion Density (kg/m3)	P/V (kW/m^3)	Np
791	13.2	0.078	2.711	933.7	2.19	0.439
828	13.8	0.078	3.346	933.7	2.70	0.472
910	15.2	0.078	4.515	933.7	3.64	0.480
968	16.1	0.078	5.397	933.7	4.48	0.477
1049	17.5	0.078	7.513	933.7	6.87	0.522

From Table 3.2 it can be seen that the power numbers for the Rushton turbine are higher than that of the 4-bladed radial disc impeller due to the slower rotational speed. The power numbers are considerably lower than those in the literature, but these depend on the mixer vessel set-up. Since the impellers are used as pump-mix impellers on the operating plant, drawing organic and aqueous into the mixing vessel (such as a centrifugal pump) as well as mixing the two phases, the impellers are installed close to the bottom of the mixer vessels. Oldshue (1983) showed that the distance off bottom of the impeller has a significant influence in the calculated power number and "proximity factors" less than 0.5 apply when the impeller is very close to the bottom of the vessel due to the throttling of suction for the bottom half of the impeller. The power number for an impeller that is installed close to the bottom of a mixing vessel, such as in these mixer-setters can therefore be of an order of magnitude less than the same impeller installed one third from the bottom as is generally found in the literature.

3.2.2 Mixing

Before the main experiments could be commenced a set of experiments was done to determine whether the pilot scale mixer-settler has the same mean residence time distribution as the PMR

plant and also to determine the effect of higher rotational speeds on the entrainment of air and therefore a reduction in effective mixer vessel volume. Three tests were done at 1000, 1100 and 1300 RPM using a 4-bladed radial disc impeller. Moirs red food colourant that is only miscible in the aqueous phase was injected into the mixer vessel after a good organic and aqueous dispersion was obtained. Samples from the mixer-settler were taken at regular intervals and were submitted for UV-vis analyses. From the UV-vis analyses concentration of the colourant versus time was plotted and the residence time distribution and mean residence time calculated at each of the different impeller rotational speeds. The relative food colourant concentration profiles using the 4-bladed radial disc impeller are illustrated in Figure 3.7. The lower concentration profile obtained at the impeller speed of 1300 RPM is due to a decrease in the effective mixing vessel volume as a result of excessive air entrainment.

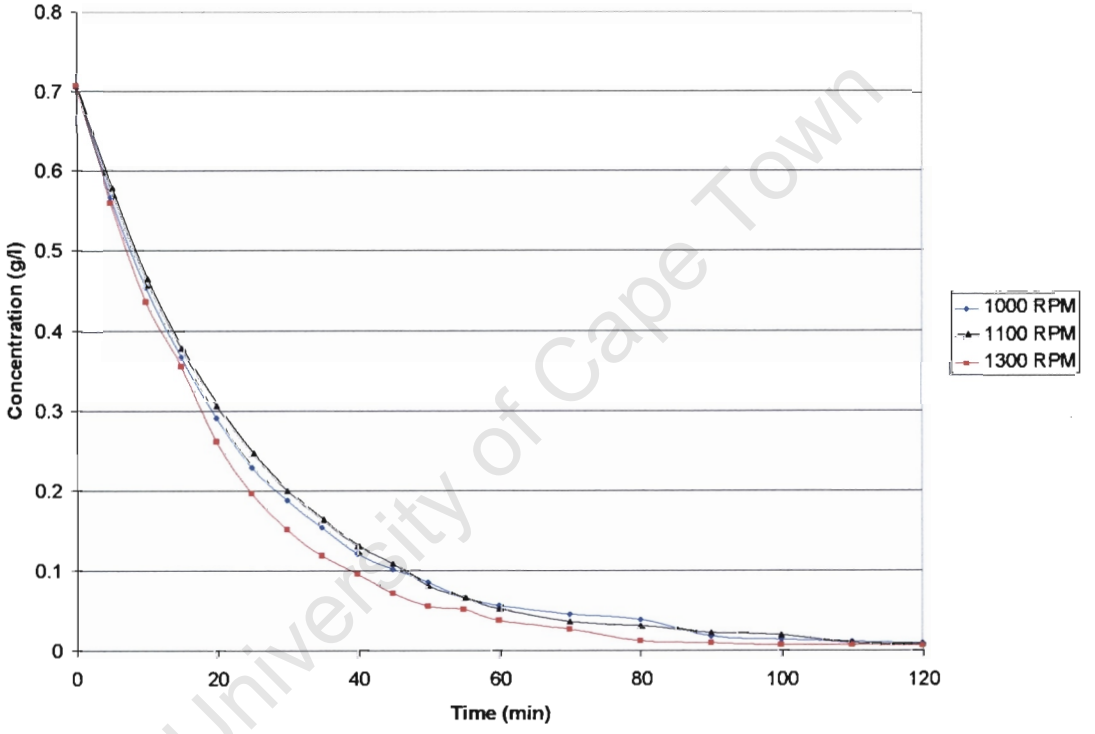

Figure 3-7 Tracer concentration profiles using a 4-bladed radial disc impeller.

The concentration profiles in Figure 3.7 are comparable to that of an ideally mixed CSTR indicating well mixed conditions and good macro-mixing. The Residence time distribution functions can be seen in appendix B and the mean residence times are highlighted in Table 3.3. It should be noted that that at 1300 RPM the strip acid mean residence time is approximately 20% lower than the mean residence time at 1100 RPM highlighting excessive air entrainment.

Table 3-3 Mean residence time for selected impeller speeds.

Impeller speed (RPM)	Mean Residence Time (min)
1000	22.62
1100	22.38
1300	18.35

3.2.3 Mass Transfer

Figure 3.8 illustrates the equilibrium palladium concentrations in the organic phase at different impeller speeds using a 4-bladed radial disc impeller and a Rushton turbine. The organic concentration decreases with an increase in impeller speed up to a certain point where air entrainment starts to play a roll as a result of vortex formation when the radial disc is used. It is at this point where a sudden drop in the effective mixing vessel volume results in a lower mean residence time and RTD and therefore decreases the efficiency of the mixer vessel resulting in a lower mass transfer of palladium from the organic phases to the aqueous phase. The organic concentration decreases with an increase in impeller speed when the Rushton turbine is used although high air entrainment and vortexing is experienced throughout the RPM range under review. The experimental data is attached in appendix B.

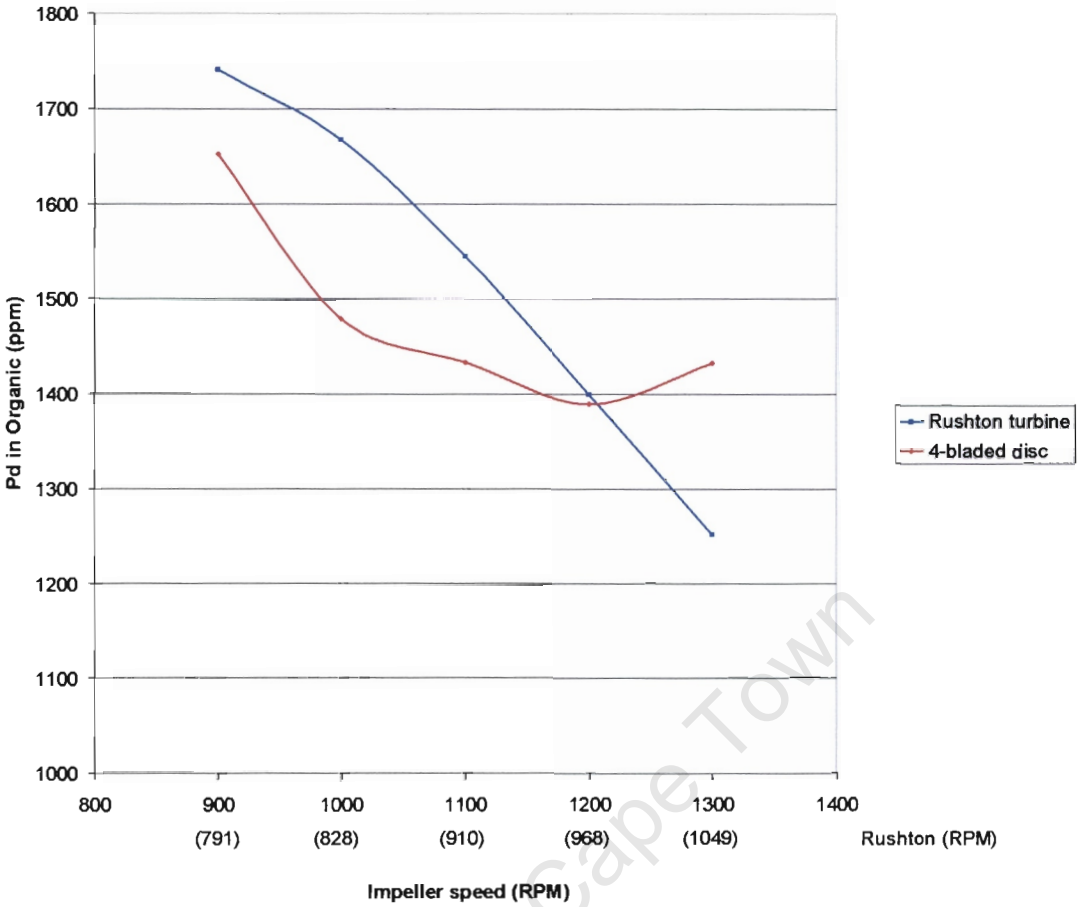

Figure 3-8 Pd in the organic phase as a function of impeller speed.

3.2.4 Overall Volumetric Mass Transfer Coefficient (K_La)

To determine the overall volumetric mass transfer coefficient (K_La), Equation 1.15 should be used for the continuous mixer-settler system.

$$Q_{aq} \cdot C_{aq_{out}} = K_L a \, (C_{org_{out}} - D_c \cdot C_{aq_{out}}) V_{eff}$$

The distribution coefficient (D_c) to be used in the above equation was obtained from the equilibrium isotherm as illustrated in Figure 3.3 (cf. Section 3.1.3).

The calculations are highlighted in appendix B and the results can be seen in Figure 3.9.

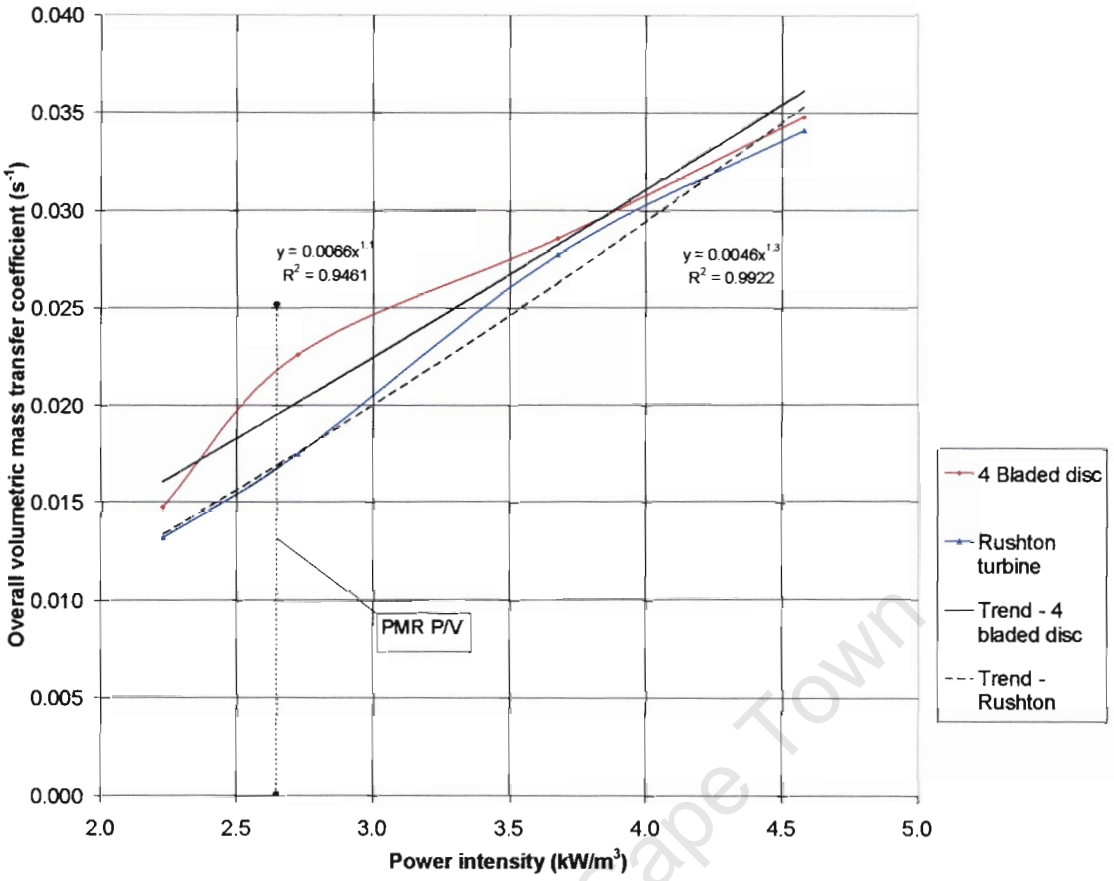

Figure 3-9 Volumetric mass transfer coefficient (K_La) as a function of power intensity (P/V).

The conclusions that can be drawn from Figure 3.9 with regard to impeller speed and type are as follows:

Impeller type - No real difference exists between the Rushton turbine and the 4-bladed radial disc impeller with regard to the overall volumetric mass transfer coefficient at equivalent power intensities.

Impeller speed - The power intensity has an overriding effect on the overall volumetric mass transfer coefficient since there is a clear increase in K_La with an increase in impeller speed. Since the value of K_La is the product of K_L and a, the only way to assess the impact of each of the two parameters on the overall volumetric mass transfer coefficients for the Rushton turbine and the 4-bladed radial disc impeller is to measure the drop sizes, but this was not done as part of this study.

The relationship between the volumetric mass transfer coefficient (K_La) and the power intensity (P/V) can be approximated by a function of the form: $Y = a X^{b}$. The data was fitted using DataFit version 8.0 software from Oakdale Engineering and the functions are as follows:

For the 4-bladed radial disc impeller:

$$K_L a = 6.6x10^{-3}\left(\frac{P}{V}\right)^{1.1}, \qquad R^2 = 0.946 \tag{3.2}$$

and for the Rushton turbine:

$$K_L a = 4.6x10^{-3}\left(\frac{P}{V}\right)^{1.3}, \qquad R^2 = 0.992 \tag{3.2}$$

Although the R^2 value is not very close to unity for both the impeller types, the power of 1.1 and 1.3 in the $K_L a$ equation corresponds well to the values reported by Moucha *et al* (2003), which lie between 0.88 and 1.25.

The trends in Figure 3.9 show that, at standard operating conditions (25°C, 6N HCl), the palladium stripping reaction is mass transfer limited over the full range of power intensities, some of which are higher than used in industry. This suggests that the stripping of palladium by solvent extraction as used in industry is mass transfer limited and can be improved by higher power intensities by increasing the impeller rotational speeds.

4 Conclusions

The objective of this thesis was to perform an investigation into the effect of hydrodynamic parameters, driven by the central hydrodynamic variables of impeller speed and type, on the stripping of palladium from a typical loaded palladium organic. The conclusions regarding the findings of this thesis are presented in this chapter. They refer to results obtained from the 1/5 scale palladium mixer-settler pilot plant test work at the Anglo Platinum Research Laboratories (ARC). The conclusions presented here are broken down into stripping characterization and hydrodynamic characterization conclusions in Sections 4.1 and 4.2 respectively.

4.1 Stripping Characterization

The results for the palladium stripping characterization section of the study were obtained through an experimental test work program and the subsequent assay, mass balancing and regression analyses of the data. The results were used to plot a number of relationships. The following conclusions were drawn based on these results.

Palladium stripping characterization

- The stripping rate of palladium from the typical palladium loaded organic increases with an increase in temperature from 15°C to 35°C.
- The stripping rate of palladium from the typical palladium loaded organic increases with an increase in strip acid concentration from 4N HCl to 6N HCl.
- The palladium stripping reaction is relatively fast and approaches equilibrium within 20 minutes when 5.5N or 6N strip acid is used at temperatures above 25°C
- 93.5% stripping in a single stage can be obtained with 6N HCl at 25°C, but this value drops to 60.9% with 4N HCl at 25°C.
- The palladium stripping isotherm with 6N HCl and 25°C can be approximated by the following equation: $Pd_{org} = 0.0876 Pd_{aq}^{0.677}$ with and average distribution coefficient equal to 0.033.

4.2 Hydrodynamic Characterization

The results for the hydrodynamic characterization section of the study were obtained through a variety of techniques, including experimental measurements (e.g. torque and rotation speed) and

calculations based on experimental variables (power numbers and overall volumetric mass transfer coefficients). These results were interpreted, where possible, with reference to the major hydrodynamic variables of impeller speed and type.

Power intensity

- Power intensities ranged from 2.2 kW/m^3 to 6.9 kW/m^3 at impeller rotational speeds of 900 RPM to 1300 RPM for a 4-bladed radial disc impeller and 791 RPM and 1049 RPM for a Rushton turbine.
- Power intensities increased with increasing impeller speed for both the Rushton turbine and the 4-bladed radial disk impeller.

Mixing

- Residence time distribution (RTD) tests were performed on the 1/5 scale mixer-settler using the 4-bladed radial disc impeller at various impeller speeds. The mean residence time for impeller speeds at 1000 RPM and 1100 RPM is around 22 minutes, but drops to 18 minutes at 1300 RPM due to air entrainment as a result of vortex formation.
- All tests conducted with the Rushton turbine at equivalent power intensities as the 4-bladed radial disc impeller resulted in excessive air entrainment of up to 20% of the mixer vessel volume.
- The mean residence time of 22 minutes compares well with the operating plant mean residence time.
- Although mixing was not explicitly characterized the ranges of power intensities, impeller rotational speeds and lack of phase separation in the mixer vessel indicated that the mixing vessel was well mixed, both in terms of macro and micro-mixing.

Mass transfer

- Palladium stripping from the loaded organic increased with an increase in impeller speed up to about 1200 RPM with the 4-bladed radial disc impeller, where after air entrainment resulted in the stripping becoming worse mainly due to a decrease in mean residence time.
- Palladium stripping, using a Rushton turbine, from the loaded organic increased with an increase in impeller speed up to 1300 RPM notwithstanding excessive air entrainment and surging action of the effective mixer vessel volume.
- The overall volumetric mass transfer coefficient (K_La), using a 4-bladed radial disc impeller and Rushton turbine, was found to be between 0.013 s^{-1} and 0.035 s^{-1} at the impeller speeds under review.

- The overall volumetric mass transfer coefficient increased with an increase in impeller speed and power intensity, but decreased again as soon as air was entrained due to vortex formation in the case of the 4-bladed radial disc impeller.

In general, the results tend to follow the types of trends observed in the solvent extraction literature. This includes an increase in palladium stripping rate due to an increase in temperature and strip acid normality. An increase in impeller speed also has a positive effect on the overall stripping rate based on the increase in the overall volumetric mass transfer coefficient.

Based on all of the above conclusions it should be concluded that the PMR palladium mixer-settler stripping impellers should be run at higher impeller speeds utilizing the higher overall volumetric mass transfer coefficients obtainable and thereby allowing increased throughput and stage efficiencies. This said, it should be born in mind that there might be phase disengagement limitations in the settlers as a result of the enhanced mixing although this was not evident during the test work when "fresh" organic was used.

REFERENCES

1. Barnes, J.E. and Edwards, J.D., 1982, Solvent extraction at Inco's Acton precious metals refinery, Chemistry & Industry, (5) pp.151 – 155.

2. Bridges, D.W. and Rosenbaum, J.B., 1962. Metallurgical application of solvent extraction – Fundamentals of the process. United States Department of the Interior. Bureau of Mines.

3. Charlesworth, P., 1981. Separating the platinum group metals by liquid-liquid extraction. Platinum Metals Review. 25, (3) 106-112

4. Cleare, M.J., Charlesworth, P. and Bryson, D.J., 1979. Solvent extraction in platinum group metal processing. J. Chem. Tech. Biotech., 29, p 210-214.

5. Clemson university website, 2004. Agitation.
http://www.ces.clemson.edu/chemeng/undergraduate/uolab/agitatio.htm

6. Cole P.M., 1994. Review of, and advances in, solvent extraction technology. SAIMM Hydrometallurgy School, Mintek, Randburg, South Africa, 27-29 Jul 1994, Johannesburg, South African Institute of Mining and Metallurgy.

7. Deglon, D.A., Egya-Mensah, D. and Franzidis, J-P, 2000. Review of hydrodynamics and gas dispersion in flotation cells on South African platinum concentrators. Miner. Eng., 13: 235-244.

8. Deglon, D.A., 2004. Personal communication.

9. Edwards, R.I., 1975. The refining of platinum-group metals. National Institute for Metallurgy Report no. 1744

10. Flett, D.S., 1982. Solvent extraction in hydrometallurgy. Hydrometallurgy Research, Development and Plant Practice. Osseo-Asare, K. and Miller, J.D. (eds). The Metallurgical Society, Warrendale, P.A.

11. Flett, D.S., Melling, J. and Cox, M., 1983. Commercial solvent systems for inorganic processes. Handbook of Solvent Extraction, T.C. Lo; Baird, M.H.I. and Hanson, C. (eds). John Wiley and Sons, New York.

12. Fox, M.H. and Feather A.M., 1994. Solvent extraction miniplants. SAIMM Hydrometallurgy School, Mintek, Randburg, South Africa, 27-29 Jul 1994, Johannesburg, South African Institute of Mining and Metallurgy.

13. Godfrey, J.C., Slater, M.J., 1994. Liquid-Liquid Extraction Equipment. John Wiley & Sons Ltd. pp 54-55.

14. Grant, R.A., Smith, C.S., Boyd, D.A., 1998. PMR Teach-in slide presentation by JMTC and ARC at Hexriver. Confidential in-house document -Anglo Platinum Research Center Library.

15. Harris, B.F., 1993. A review of precious metal refining, Precious Metals 1993, International Precious Metals Institute, Allentown, PA, pp. 351 – 374.

16. Kennedy, B., Davenport, W.G., Jenkins and Robinson, T., 1999. Electrolytic copper electrowinning and solvent extraction – world operating data. Proceedings Society of Mining and Exploration Annual Meeting, Denver, pp. 41-87.

17. Linek, V., Moucha, T., Fujasova, M. and Prokopova, E., 2002. Energy demands of different impeller types in gas-liquid dispersions, Proceedings of the 9th APCChE Congress and CHEMECA 2002, 29 September-3 October 2002, Christchurch, NZ, P.A.Gostomski and K.R. Morison, eds., University of Canterbury, Christchurch, NZ, ISBN 0-473-09252-2, Paper #875.

18. Mooiman, M.B., 1993. The solvent extraction of precious metals – A review, Precious Metals 1993, International Precious Metals Institute, Allentown, PA, pp. 411 – 434.

19. Moucha, T., Linek, V., Prokopova, E., 2003. Gas hold-up, mixing time and gas-liquid volumetric mass transfer coefficient of various multiple-impeller configurations: Rushton turbine, pithed blade and techmix impeller and their combinations. Chem. Eng. Science, 58: 1839-1846.

20. Nagel, V., 1999. Basic principles involved in the design and operation of solvent-extraction systems. SAIMM SX/EW School, Johannesburg, South Africa, 13-14 Oct 1999.

21. Nash, K.L., A review of the basic chemistry and recent developments in trivalent f-element separations, Solvent Extraction and Ion Exchange, 11 (4), 729 – 768

22. Nienow, A.W., 2004. Break-up, coalescence and catastrophic phase inversion in turbulent contactors. Advances in Colloid and Interface Science 108-109:95-103.

23. Nicol, M., 2004. Kinetics of reactions in hydrometallurgy. http://wwwscience.murdoch.edu.au/teaching/pec247/Hydromet.pdf

24. Oldshue, J.Y., 1983. Fluid Mixing Technology. McGraw-Hill. pp 64-68.

25. Pacek, A.W., Chamsart, A., Nienow, A.W. and Bakker, A., 1999. The influence of impeller type on mean drop size and drop size distribution in an agitated vessel. Chem. Eng. Science, 54: 4211-4222.

26. Perry, R.H. and Green, D.W., 1999. Perry's Chemical Engineer's Handbook. McGraw-Hill. pp 21-62,15-24,14-1 to 14-14,4-10.

27. Podgórska, W. and Baldyga, J., 2001. Scale-up effects on the drop size distribution of liquid-liquid dispersions in agitated vessels. Chem. Eng. Science, 56: 741-746.

28. Post, T.A., 2003. http://www.postmixing.com/mixing_forum/Macro/Liq-Liq/Mixer-Settlers/Publication1/article1.htm - Introduction

29. Preston, J.S. and du Preez, A.C., 2002. Solvent extraction of platinum group metals from hydrochloric acid solutions by dialkylsulphoxides. Solvent Extraction and Ion Exchange, 20(3), 359-374.

30. Renner, H., 1985. The selective solvent extraction of palladium by the use of di-normal-hexyl sulphide, Mintek Report, No. M217.

31. Reavill, L.R.P. and Charlesworth P., 1980. The application of solvent extraction to platinum group metal refining. Proc. Int. Solvent Extraction Conf. ISEC '80, Leige, Belgium, Vol 3, p80.

32. Reeve, R.N. and Godfrey, J.C., 2002. Phase inversion during liquid-liquid mixing in continuous flow, pump mix, agitated tanks. Chem. Eng. Research and Design, Vol 80, Issue 8 864-871.

33. Rimmer, B.F., 1989, Refining of platinum group metals by solvent extraction, Precious Metals1989, B.Harris (ed.), International Precious Metals Institute, Allentown, PA, pp.217 – 226.

34. Ritcey, G.M. and Ashbrook, A.W., 1979a. Solvent extraction – principles and applications to process metallurgy handbook - Part I. Elsevier, New York. pp 40-86.

35. Ritcey, G.M. and Ashbrook, A.W., 1979b. Solvent extraction – principles and applications to process metallurgy handbook - Part II. Elsevier, New York. pp 1-41.

36. Rushton, J.H., Costich, E.W. and Everett, H.J., 1950a. Power characteristics of mixing impellers – part 1. Chem. Eng. Progress, 46: 395-404.

37. Rushton, J.H., Costich, E.W. and Everett, H.J., 1950b. Power characteristics of mixing impellers – part 2. Chem. Eng. Progress, 46: 467-476.

38. Sandler, H.J. and Luchiewicz, E.T., 1987. Practical Process Engineering – A Working Approach to Plant Design Handbook. McGraw-Hill, New York.

39. Shanton, K.J. and Grant, R.A., 1982. Solvent extraction process for the selective extraction of palladium. U.S. Patent # 4,331,634.

40 Sole, K.C., 1999. Process experience: chemical and industrial applications. Lecture 3, International Solvent Extraction School '99, Barcelona, Spain, Jul 1999.

41. Tunley, T.H. and Birch, C.P., 1970. The recovery of copper from sulphate leach liquors by liquid ion exchange with LIX-64N. National Institute of Metallurgy report no. 964.

42. Yantz, K., 2000. Choosing the proper mixer.
www.chemicalprocessing.com/web_first/cp.nsf/articleid/dgrn-4rquc3/

43. Young, G., 2001. Educ. Reso. for Part. Techn. **014Q-Young.** http://www.erpt.org/014Q/youa-00.htm

Appendix A:
Experimental data – Characterization Experiments

Strip acid palladium concentration (ppm) vs. time.

Time (min)	35°C and 6N HCl	35°C and 5.5N HCl	35°C and 5N HCl	35°C and 4.5N HCl	35°C and 4N HCl
0	0	0	0	0	0
1	32760	26360	16590	8070	2545
2	37230	32650	23070	12870	4973
3	38260	36040	27170	16520	6860
4	38260	36729	30130	19300	9191
5	39420	37709	31870	20850	10701
10	38860	38600	35570	27830	16761
30	40540	38780	38410	34760	27341
40				35840	29451
50					32061
60					
Formula	Best Fit Formula	Best Fit Formula	Best Fit Formula	Best Fit Formula	Best Fit Formula
	Y=a*X/(b+X)	Y=a*X/(b+X)	Y=a*X/(b+X)	Y=a*X/(b+X)	Y=a*X/(b+X)
	R2				
	0.99845	0.9966699	0.999403	0.99943	0.9994801
	a				
	40688.20583	40658.83254	40612.0943	39542.73238	40510.88538
	b				
	0.224204	0.489637234	1.454455667	4.213411002	14.18576928
Time (min)	Formula generate	Formula generated	Formula generate	Formula generated	Formula generated
0	0	0	0	0	0
1	33236	27294	16546	7585	2668
2	36587	32662	23513	12728	5006
3	37859	34954	27352	16446	7072
4	38529	36225	29783	19258	8910
5	38942	37032	31461	21459	10558
10	39796	38761	35455	27821	16750
20	40237	39687	37859	32662	23700
30	40386	40006	38734	34673	27505
40				35774	29905
50					31558

Time (min)	25°C and 6N HCl	25°C and 5.5N HCl	25°C and 5N HCl	25°C and 4.5N HCl	25°C and 4N HCl
0	0	0	0	0	0
1	17595.4	13614.3	7956.34	2709.43	1129.43
2	27635.4	21874.3	14265.92	5359.05	2239.43
3	32055.4	27744.3	18316.34	8504.3	3315.05
4	35545.4	30144.3	21696.34	10674.3	4249.05
5	36508.6	32304.3	24536.34	12160.5	5159.05
10	38303.8	36674.3	31375.92	20964.3	9830.5
30	39365.4	38444.3	36046.34	28944.3	19054.3
40				30890.5	21314.3
50					23244.3
60					
Formula	Best Fit Formula	Best Fit Formula	Best Fit Formula	Best Fit Formula	Best Fit Formula
	x/(a+b*x+c*sqr(x))+(	Y=a*X/(b+X)	Y=a*X/(b+X)	Y=a*X/(b+X)	Y=a*X/(b+X)
	0.999	0.998825	0.99657	0.99497	0.9993535
	5.40454.E-05	40784.06596	41399.46825	39465.15855	36909.28683
	2.88484.E-05	1.366798072	3.665688786	10.58561481	28.96020519
Time (min)	Formula generate	Formula generated	Formula generate	Formula generated	Formula generated
0	0	0	0	0	0
1	18011	17232	8873	3406	1232
2	27387	24227	14614	6271	2384
3	32201	28019	18632	8715	3465
4	34886	30397	21602	10823	4479
5	36491	32029	23887	12661	5434
10	39136	35880	30294	19171	9474
20	39603	38175	34987	25806	15077
30	39612	39007	36892	29172	18780
40				31207	21409
50				32570	23372

Time (min)	15°C and 6N HCl	15°C and 5.5N HCl	15°C and 5N HCl	15°C and 4.5N HCl	15°C and 4N HCl
0	0	0	0	0	0
1	6975	4566	2160	810	364
2	14505	9527	4640	1768	763
3	20175	14252	7055	2969	1199
4	25015	18357	10155	4107	1571
5	26765	20767	12185	5148	2057
10	33925	29637	19455	9420	4097
30	37759	35752	30337	18900	9720
40	38139	36337	32195	22270	12260
50				24450	14200
60					16000.4
Formula	Best Fit Formula	Best Fit Formula	Best Fit Formula	Best Fit Formula	Best Fit Formula
	Y=a*X/(b+X)	Y=a*X/(b+X)	Y=a*X/(b+X)	Y=a*X/(b+X)	Y=a*X/(b+X)
	0.985828	0.98977	0.996203	0.999275	0.99977
	42653.81248	42674.02903	43725.24319	42677.98224	42164.42738
	3.317196152	5.61668446	13.55797661	37.11376731	98.28907465
Time (min)	Formula generate	Formula generated	Formula generate	Formula generated	Formula generated
0	0	0	0	0	0
1	9880	6449	3004	1120	425
2	16044	11205	5621	2182	841
3	20256	14857	7922	3192	1249
4	23317	17750	9961	4152	1649
5	25642	20098	11781	5067	2041
10	32029	27326	18561	9058	3894
20	36586	33317	26060	14945	7129
30	38407	35944	30115	19077	9860
40	39387	37420	32656	22138	12196
50				24496	14217
60					15983

Palladium extraction after 20 minutes at different temperatures.

	% Pd extraction at 15°C		% Pd extraction at 25°C		% Pd extraction at 35°C	
Normality	ppm in Aqueous	Extraction	ppm in Aqueous	% Extraction	ppm in Aqueous	% Extraction
6	36586	86%	39603	93%	40237	95%
5.5	33317	79%	38175	90%	39687	94%
5	26060	62%	34987	83%	37859	89%
4.5	14945	35%	25806	61%	32662	77%
4	7129	17%	15077	36%	23700	56%

Equilibrium isotherm at 25°C and 6N HCl.

Organic stripped with 9N HCl on 10ml to 50 ml ratio (2 x 25ml HCL contacts) EXCEPT D1 is to 75 ml					
	Pd	Real Pd		Recalc to organic	
D6 ORG 10x	0.18	1.85		**9**	(10:50)
D5 ORG 10x	1.66	16.55		**83**	(10:50)
D4 ORG 10x	5.82	58.24		**291**	(10:50)
D3 ORG 10x	9.69	96.90		**484**	(10:50)
D2 ORG 10x	15.44	154.43		**772**	(10:50)
D1 ORG 10x	13.63	136.28		**1022**	(10:75)

Neat Aqueous				Recalc to Aqueous g/l	
				0.2	
D6 AQ 1000x	-0.39	-390.22		**1.0**	
D6 AQ 100x	1.28	127.97		**5.9**	
D6 AQ 10x	17.50	174.97		**12.2**	
D5 AQ 1000x	0.61	612.13		**24.9**	
D5 AQ 100x	10.24	1023.77		**37.9**	
D5 AQ 10x	101.56	1015.64			
D4 AQ 1000x	5.67	5671.48			
D4 AQ 100x	58.98	5898.08			
D4 AQ 10x	535.90	5358.98			
D3 AQ 1000x	12.24	12244.85			
D3 AQ 100x	121.81	12180.70			
D3 AQ 10x	974.21	9742.12			
D2 AQ 1000x	25.60	25600.80			
D2 AQ 100x	249.10	24910.45			
D2 AQ 10x	1602.15	16021.45			

Appendix B:

Experimental data – Hydrodynamic Characterization Experiments

Linear variables for hydrodynamic characterization experiments – 4-bladed radial disc impeller.

Variable		Meaning
T	0.108 m	Tank Diameter (L,H,W)
D	0.078 m	Impeller Diameter
H	0.108 m	Liquid Depth
C	1 mm	Impeller Height Above Tank Bottom
S	n/a	Pitch of the Impeller
L	0.108 m	Length of Impeller Blade
W	4 mm	Width of Impeller Blade
J	n/a	Baffle Width
B	4	Number of Blades on Impeller
R	n/a	Number of Baffles

Linear variables for hydrodynamic characterization experiments – Rushton turbine.

Variable		Meaning
T	0.108 m	Tank Diameter (L,H,W)
D	0.078 m	Impeller Diameter
H	0.108 m	Liquid Depth
C	1 mm	Impeller Height Above Tank Bottom
S	n/a	Pitch of the Impeller
L	0.108 m	Length of Impeller Blade
W	4 mm	Width of Impeller Blade
J	n/a	Baffle Width
B	6	Number of Blades on Impeller
R	n/a	Number of Baffles

Experimental data for 4-bladed radial disc impeller.

Impeller	rpm	PMR 900	PMR 1000	PMR 1100	PMR 1200	PMR 1300
Mass initial	kg	0.433	0.433	0.433	0.433	0.433
Mass end	kg	0.373	0.367	0.352	0.343	0.319
Mass diff.		0.060	0.066	0.081	0.090	0.114
g		9.810	9.810	9.810	9.810	9.810
F=	N	0.589	0.647	0.795	0.883	1.118
Distance	m	0.050	0.050	0.050	0.050	0.050
Torque	Nm	0.029	0.032	0.040	0.044	0.056
RPM	rpm	900.000	1000.000	1100.000	1200.000	1300.000
P=	watt	2.763	3.377	4.558	5.525	7.582
V=	m3	0.001	0.001	0.001	0.001	0.001
P/V	kw/m3	2.228	2.723	3.676	4.581	6.934
T/S calcs						
Diameter	mm	78.000	78.000	78.000	78.000	78.000
	m	0.078	0.078	0.078	0.078	0.078
Tipspeed	m/s	3.676	4.084	4.492	4.901	5.309

Experimental data for Rushton turbine impeller.

Impeller	rpm	Rushton 791	Rushton 828	Rushton 910	Rushton 968	Rushton 1049
Mass initial	kg	0.438	0.438	0.438	0.438	0.438
Mass end	kg	0.371	0.359	0.341	0.329	0.298
Mass diff.		0.067	0.079	0.097	0.109	0.140
g		9.810	9.810	9.810	9.810	9.810
F=	N	0.657	0.775	0.952	1.069	1.373
Distance	m	0.050	0.050	0.050	0.050	0.050
Torque	Nm	0.033	0.039	0.047	0.053	0.068
RPM	rpm	791.000	828.000	910.000	968.000	1049.000
P=	watt	2.711	3.346	4.516	5.398	7.513
V=	m3	0.001	0.001	0.001	0.001	0.001
P/V	kw/m3	2.187	2.699	3.642	4.475	6.871
P/V Difference to PM		1.86%	0.89%	0.93%	2.30%	0.90%
T/S calcs						
Diameter	mm	78.000	78.000	78.000	78.000	78.000
	m	0.078	0.078	0.078	0.078	0.078
Tipspeed	m/s	3.230	3.382	3.717	3.953	4.284

Volumetric mass transfer calculations for 4-bladed radial disc impeller.

Impeller rpm		PMR 900	PMR 1000	PMR 1100	PMR 1200	PMR 1300
Pd	g/mol	106.4	106.4	106.4	106.4	106.4
Organic	ratio	155	155	155	155	155
Aqueous	ratio	45	45	45	45	45
Mixer vol	ml	1240	1240	1240	1240	1240
Mixer vol	m3	0.00124	0.00124	0.00124	0.00124	0.00124
Veffective	ml	1240.000	1240.000	1240.000	1240.000	1093.455
Veffective	m3	0.001240	0.001240	0.001240	0.001240	0.001093
Res time	min	21.488	21.488	21.488	21.488	18.948
Qtotal	m3/min	5.77E-05	5.77E-05	5.77E-05	5.77E-05	5.77E-05
Qtotal	m3/s	9.62E-07	9.62E-07	9.62E-07	9.62E-07	9.62E-07
Qaq	m3/s	2.16E-07	2.16E-07	2.16E-07	2.16E-07	2.16E-07
Caqin	ppm	0	0	0	0	0
Caqin	mol/m3	0	0	0	0	0
Caqout	ppm	36935.47	36342.70	36655.10	36567.57	36705.03
Caqout	g/l	36.94	36.34	36.66	36.57	36.71
Caqout	mol/m3	347.07	341.50	344.44	343.62	344.91
D	from eq	0.033	0.033	0.033	0.033	0.033
Corg out	ppm	1652.76	1478.96	1433.00	1389.86	1432.32
Corg out	g/l	1.65	1.48	1.43	1.39	1.43
Corg out	mol/m3	15.53	13.90	13.47	13.06	13.46
Caqout	g/l	36.94	36.34	36.66	36.57	36.71
Caqout	mol/m3	347.07	341.50	344.44	343.62	344.91
LH		7.51071E-05	7.39018E-05	7.4537E-05	7.4359E-05	7.46386E-05
RH		0.00506	0.00326	0.00260	0.00213	0.00227
Kla	1/s	0.01486	0.02268	0.02864	0.03485	0.03286

Volumetric mass transfer calculations for Rushton turbine.

Mixer vol	ml	1240	1240	1240	1240	1240
Mixer vol	m3	0.00124	0.00124	0.00124	0.00124	0.00124
Veffective	ml	969.455	969.455	958.182	1240.000	913.091
Veffective	m3	0.000969	0.000969	0.000958	0.001240	0.000913
Res time	min	16.800	16.800	16.604	21.488	15.823
Qtotal	m3/min	5.77E-05	5.77E-05	5.77E-05	5.77E-05	5.77E-05
Qtotal	m3/s	9.62E-07	9.62E-07	9.62E-07	9.62E-07	9.62E-07
Qaq	m3/s	2.16E-07	2.16E-07	2.16E-07	2.16E-07	2.16E-07
Caqin	ppm	0	0	0	0	0
Caqin	mol/m3	0	0	0	0	0
Caqout	ppm	34780.00	35794.00	36846.00	37259.00	37361.00
Caqout	g/l	34.78	35.79	36.85	37.26	37.36
Caqout	mol/m3	326.82	336.35	346.23	350.12	351.07
D	from eq	0.033	0.033	0.033	0.033	0.033
Corg out	ppm	1730.00	1636.00	1515.00	1473.00	1450.00
Corg out	g/l	1.73	1.64	1.52	1.47	1.45
Corg out	mol/m3	16.26	15.37	14.24	13.84	13.63
Caqout	g/l	34.78	35.79	36.85	37.26	37.36
Caqout	mol/m3	326.82	336.35	346.23	350.12	351.07
LH		7.07249E-05	7.27861E-05	7.49258E-05	0.000075766	7.59721E-05
RH		0.00530	0.00414	0.00269	0.00222	0.00186
Kla	1/s	0.01333	0.01757	0.02783	0.03417	0.04079

Residence Time Distribution (RTD) for 4-bladed radial disc impeller at 1000 RPM.

Time (minutes)	C(t) Mg	N = 30 h = (150-0)/30 = 5 h = interval	integration 5 minute interval	E(t) = C(t)/area E(t)	Time (minutes)	t.E(t)	N = h = (180-0 inte	t.E(t) integration 5 minute interval
0	0.702	1	1.32	0.04	0	0.000	1	0.00
5	0.561	3	3.16	0.04	5	0.177	3	1.00
10	0.448	3	2.52	0.03	10	0.283	3	1.59
15	0.361	2	1.35	0.02	15	0.342	2	1.28
20	0.285	3	1.60	0.02	20	0.360	3	2.02
25	0.223	3	1.25	0.01	25	0.352	3	1.98
30	0.182	2	0.68	0.01	30	0.345	2	1.29
35	0.148	3	0.83	0.01	35	0.327	3	1.84
40	0.115	3	0.65	0.01	40	0.291	3	1.63
45	0.096	2	0.36	0.01	45	0.273	2	1.02
50	0.079	3	0.44	0.00	50	0.249	3	1.40
55	0.060	3	0.34	0.00	55	0.208	3	1.17
60	0.050	1	0.09	0.00	60	0.189	1	0.36
60	0.050	1	0.19	0.00	60	0.189	1	0.71
70	0.039	3	0.44	0.00	70	0.172	3	1.94
80	0.032	3	0.36	0.00	80	0.162	3	1.82
90	0.012	2	0.09	0.00	90	0.068	2	0.51
100	0.008	3	0.09	0.00	100	0.051	3	0.57
110	0.005	3	0.06	0.00	110	0.035	3	0.39
120	0.003	1	0.01	0.00	120	0.023	1	0.09
		integr. 5' interval:	15.83			mean res. time:		22.622 minutes

Time (minutes)	) = C(t)/a E(t)	h = (20-0)/4 = 5 h = interval	0-20 E(t) integrate
0	0.04	1	0.0739
5	0.04	4	0.2362
10	0.03	2	0.0943
15	0.02	4	0.1520
20	0.02	1	0.0300
		0-60 integrate:	0.5864
			58.64%

Time (minutes)	E(t) = C(t)/area E(t)	0-0 inte	0-25 E(t) integrate
0	0.04	1	0.0739
5	0.04	4	0.2362
10	0.03	2	0.0943
15	0.02	4	0.1520
20	0.02	2	0.0600
25	0.01	4	0.0939
30	0.01	1	0.0192
	0-60 integrate:		0.7294
			72.94%

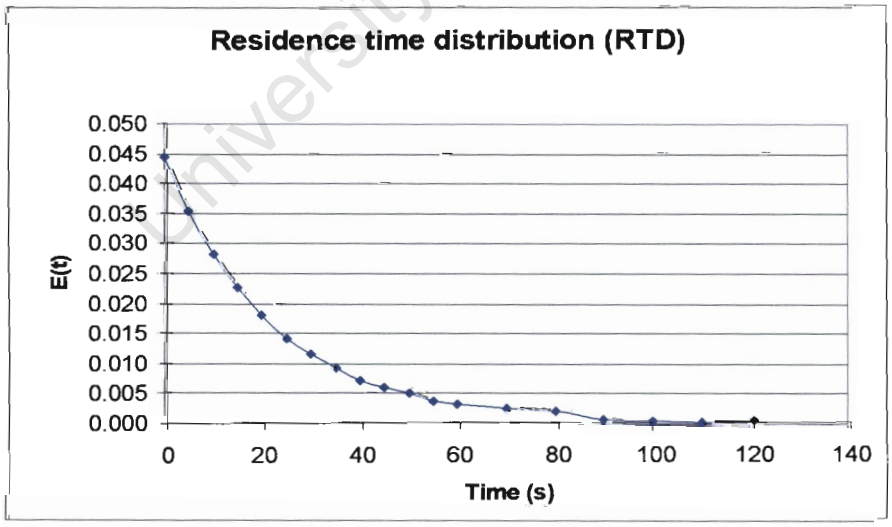

Residence Time Distribution (RTD) for 4-bladed radial disc impeller at 1100 RPM.

Time (minutes)	C(t) Mg	N = 30 h = (150-0)/30 = 5 h = interval	integration 5 minute interval	E(t) = C(t)/area E(t)	Time (minutes)	t.E(t)	N = h = (180-0 inte	t.E(t) integration 5 minute interval
0	0.755	1	1.42	0.04	0	0.000	1	0.00
5	0.616	3	3.47	0.04	5	0.176	3	0.99
10	0.494	3	2.78	0.03	10	0.283	3	1.59
15	0.401	2	1.50	0.02	15	0.344	2	1.29
20	0.323	3	1.82	0.02	20	0.370	3	2.08
25	0.259	3	1.46	0.01	25	0.370	3	2.08
30	0.209	2	0.78	0.01	30	0.359	2	1.35
35	0.170	3	0.96	0.01	35	0.340	3	1.91
40	0.134	3	0.75	0.01	40	0.307	3	1.72
45	0.111	2	0.42	0.01	45	0.286	2	1.07
50	0.081	3	0.46	0.00	50	0.232	3	1.30
55	0.065	3	0.37	0.00	55	0.205	3	1.15
60	0.050	1	0.09	0.00	60	0.172	1	0.32
60	0.050	1	0.19	0.00	60	0.172	1	0.64
70	0.033	3	0.37	0.00	70	0.132	3	1.49
80	0.027	3	0.30	0.00	80	0.124	3	1.39
90	0.018	2	0.14	0.00	90	0.093	2	0.70
100	0.015	3	0.17	0.00	100	0.086	3	0.97
110	0.004	3	0.05	0.00	110	0.025	3	0.28
120	0.002	1	0.01	0.00	120	0.014	1	0.05
		Integr. 5' interval:	17.48			mean res. time:		22.380 minutes

Time (minutes)	= C(t)/a E(t)	h = (20-0)/4 = 5 h = Interval	0-20 E(t) integrate
0	0.04	1	0.0720
5	0.04	4	0.2349
10	0.03	2	0.0942
15	0.02	4	0.1529
20	0.02	1	0.0308
		0-60 integrate:	0.5848
			58.48%

Time (minutes)	E(t) = C(t)/area E(t)	0-0 inte	0-25 E(t) integrate
0	0.04	1	0.0720
5	0.04	4	0.2349
10	0.03	2	0.0942
15	0.02	4	0.1529
20	0.02	2	0.0616
25	0.01	4	0.0988
30	0.01	1	0.0199
	0-60 integrate:		0.7343
			73.43%

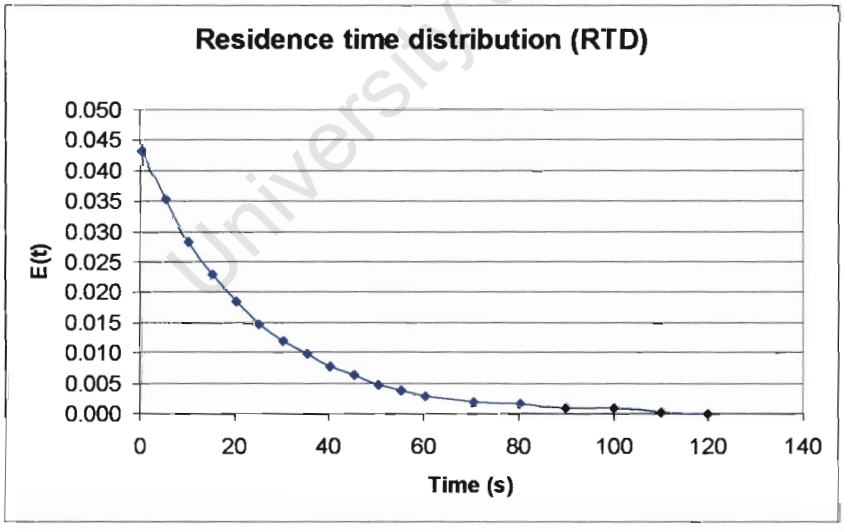

Residence Time Distribution (RTD) for 4-bladed radial disc impeller at 1300 RPM.

Time (minutes)	C(t) Mg	N = 30 h = (150-0)/30 = 5 h = interval	integration 5 minute interval	E(t) = C(t)/area E(t)	Time (minutes)	t.E(t)	N = 3 h = (180-0) inte	t.E(t) integration 5 minute interval
0	0.741	1	1.39	0.05	0	0.000	1	0.00
5	0.585	3	3.29	0.04	5	0.202	3	1.14
10	0.454	3	2.55	0.03	10	0.314	3	1.77
15	0.370	2	1.39	0.03	15	0.384	2	1.44
20	0.270	3	1.52	0.02	20	0.374	3	2.10
25	0.201	3	1.13	0.01	25	0.348	3	1.96
30	0.153	2	0.57	0.01	30	0.318	2	1.19
35	0.119	3	0.67	0.01	35	0.288	3	1.62
40	0.095	3	0.53	0.01	40	0.263	3	1.48
45	0.070	2	0.26	0.00	45	0.218	2	0.82
50	0.053	3	0.30	0.00	50	0.183	3	1.03
55	0.048	3	0.27	0.00	55	0.183	3	1.03
60	0.034	1	0.06	0.00	60	0.141	1	0.26
60	0.034	1	0.13	0.00	60	0.141	1	0.53
70	0.022	3	0.25	0.00	70	0.107	3	1.20
80	0.007	3	0.08	0.00	80	0.039	3	0.44
90	0.004	2	0.03	0.00	90	0.025	2	0.19
100	0.001	3	0.01	0.00	100	0.007	3	0.08
110	0.001	3	0.01	0.00	110	0.008	3	0.09
120	0.000	1	0.00	0.00	120	0.000	1	0.00
		integr. 5' interval:	14.45			mean res. time:		18.354 minutes

Time (minutes)	= C(t)/a E(t)	h = (20-0)/4 = 5 h = interval	0-20 E(t) integrate
0	0.05	1	0.0855
5	0.04	4	0.2699
10	0.03	2	0.1047
15	0.03	4	0.1707
20	0.02	1	0.0311
		0-60 integrate:	0.6620
			66.20%

Time (minutes)	E(t) = C(t)/area E(t)	0-0 inte	0-25 E(t) integrate
0	0.05	1	0.0855
5	0.04	4	0.2699
10	0.03	2	0.1047
15	0.03	4	0.1707
20	0.02	2	0.0623
25	0.01	4	0.0927
30	0.01	1	0.0176
	0-60 integrate:		0.8035
			80.35%